Fall 12-17-2021

Metabolic heterogeneity and the roles of CodY and CcpA in central metabolism and S. aureus biofilm formation.

Logan L. Bulock
University of Nebraska Medical Center

Metabolic heterogeneity and the roles of CodY and CcpA in central metabolism and *S. aureus* biofilm formation.

by

Logan Bulock

A DISSERTATION

Presented to the Faculty of
the University of Nebraska Graduate College
in Partial Fulfillment of the Requirements
for the Degree of Doctor of Philosophy

Pathology & Microbiology Graduate Program

Under the Supervision of Professor Kenneth W. Bayles

University of Nebraska Medical Center
Omaha, Nebraska

December 2021

Supervisory Committee:

Paul Fey, PhD
Vinai Thomas, PhD
Simon Foster, PhD
Laurey Steinke, PhD
Marat Sadykov, PhD

Acknowledgements

There are many people I need to thank for all of the help and support I've received through my years as a graduate student. First and foremost, I'd like to thank my wife, Chelsea. Without your love and support, I wouldn't have made it to the finish line. Your support, love, and encouragement has pushed me to be a better person, a better scientist, and a better father. You're the best partner I could ever dream of growing old with. You and Leo mean the world to me, and I am so excited to see what the next chapters of our lives bring us.

Next, I'd like to thank my parents, Gene and Michele, for the love and support they've given me throughout my entire life. Thank you for providing an environment to thrive and grow into my own person and for being such great role models in life.

I'd also like to thank the people who helped train me in the laboratory: Jennifer, Derek, Rebecca, and Marat. Your guidance was a blessing and I'm forever in gratitude for welcoming me into the Bayles (and Foster) laboratory and for the supportive environment to hone my skills as a scientist. I'd also like to acknowledge some great friends I've made during my time in the Bayles lab: Janani, Ben, VJ, and Sam. Graduate school is where I became addicted to coffee and it's in no small part thanks to you all. I'll cherish the memories, conversations, and fun we had.

Of course, I need to thank my mentor, Ken, for his support and training throughout these years. You've helped me overcome some of my biggest weaknesses and turn them into strengths. Your unwavering support, especially in my times of struggle, meant a lot to me.

Finally, I'd like to thank my supervisory committee members for guiding me on my PhD journey. It was always evident that each one of you cared about me as a student, a scientist, and a person.

Abstract

Staphylococcus aureus is a metabolically versatile human pathogen, causing disease in many areas of the body. Its versatility can be attributed to the fact that it utilizes a variety of tools to adapt to many different environments, including toxins to scavenge from the host and multiple transporters to compete for its preferred carbon sources. *S. aureus* can also survive in harsh conditions through biofilm development, which are notoriously recalcitrant to antibiotics and immune defenses. Biofilms exhibit marked heterogeneity, with division of labor for production of matrix components and differential gene expression among various niches within the biofilm.

In this study, we investigated the development of metabolic heterogeneity as structures form during biofilm maturation. Additionally, we investigated how metabolic regulators control proper development of mature structures and their impact on biofilm matrix composition. We observed the initiation of metabolic heterogeneity before nutrient gradients could form within structures, consistent with recent findings that heterogeneity is a trait that begins from the first stages of biofilm development, when cells encounter a surface. Furthermore, we observed inactivation of CodY and CcpA have a substantial impact on central carbon and nitrogen metabolism as well as toxin production and biofilm development.

Table of Contents

Table of Figures

List of Tables

1 Literature Review

1.1 Biofilm development is an intricate process marked by heterogenic gene expression, matrix production, and other behaviors.

Biofilms have long been observed, with the earliest documentation in 1933 by Arthur Henrici, who characterized biofilm growth on submerged surfaces (1). During the 1980s, a greater appreciation for biofilms was realized when bacterial life in streams was found to be predominantly in the form of biofilms (2). Not long after, it was postulated that biofilms develop in a regulated developmental process (3). Indeed, much evidence has been found to support the notion that microbes follow a largely conserved developmental process that progresses in multiple stages, though there is still much to be learned.

In contrast to their planktonic counterparts, biofilms are surface attached, structured communities that are encased in an extracellular matrix (ECM) comprised of a combination of exopolysaccharides, proteins, and nucleic acids (4). Bacteria may form biofilms as a way to survive stressors in rapidly changing environmental conditions. The first known fossils of ancient microorganisms were found in what were sub-marine hydrothermal vents from at least 3,770 million years ago (5). In fact, the evolution of Earth's earliest life-forms has been proposed to occur near these hydrothermal vents, where reduced hydrothermal fluids mix with seawater to provide an energy-rich environment and substrates required for metabolic reactions (6). To this day, these hydrothermal vents support abundant microbial life, whereas the rest of the deep-sea floor is desolate (7). At these hydrothermal vents, microorganisms utilize the sulfur cycle

for energy, using ferric and sulfuric minerals from the vents for oxidation reactions (8-10).

Since nearly all microbial life is found in the biofilm form in nature and the first known microorganisms were found in microbial mats, perhaps biofilm-forming microbes were selected for on primordial planet Earth. Biofilm formation would allow microorganisms to adhere to a surface and persist near a nutrient source, providing an advantage in rapidly changing environments (5, 11-13). Given the challenging and inhospitable origins of biofilms, it is not surprising that “modern” biofilms are resistant to starvation, immune defenses, and antimicrobial agents (14-18).

In addition to resistance to stressful conditions, the hydrothermal vents of our primordial Earth likely helped drive biofilm evolution in another way: toward the heterogeneity and division of labor that are essential for maximizing fitness of the species. Bacteria grown in their natural biofilm form display marked heterogeneity, from task allocation and specialized matrix-producers to subpopulations of antibiotic-tolerant cells (19, 20). Historically, studies of bacteria were conducted only in the context of planktonic cultures measuring averages within the population, completely overlooking the primary mode of bacterial growth (biofilm) and overlooking differences among the individuals in the population. In other words, we were trying to make sense of these complex organisms by averaging the characteristics of cells growing in planktonic culture, rather than examining the interactions and diversity of individuals living within a community. Imagine trying to understand organ systems by studying cultured cells. We would likely learn a great deal about the growth characteristics of these cells, but completely miss the intricate details of the communal behavior that is essential to their ultimate function, and to the survival of the whole organism. Yet despite taking cells out of their natural form of growth, planktonic cells still exhibit marked heterogeneity

suggesting the processes eliciting heterogenic behavior are deeply engrained in the functionality of the cell (21).

Understanding the developmental processes driving biofilm formation will aid in the discovery of new anti-biofilm therapeutics. In the following section, I will discuss the current understanding of the *S. aureus* biofilm developmental process.

1.1.1 Stages of biofilm development

Once thought of as merely a collection of cells, more or less randomly organized within a matrix, biofilm development is now known to be an intricate process culminating in the formation of complex multicellular structures with common features shared among most microorganisms, such as differential gene expression, physiological heterogeneity, and division of labor. The complexity of these structures manifest in multiple ways, including the formation of fruiting bodies, microcolonies, and floating aggregates, depending on the environment and characteristics of the organism. For example, motile bacteria like *Bacillus subtilis* and *Myxococcus xanthus* form stalk-like structures called fruiting bodies, which can become hot spots for spore formation (22, 23). Other bacteria simply form mounds or “towers” that are often referred to as “microcolonies” (24).

S. aureus biofilms develop in 5 stages: attachment, multiplication, exodus, maturation, and dispersal (25), as depicted in Figure 3 and outlined below.

Attachment. The first step of the developmental process is to attach to a surface, which can provide several benefits to an organism. First, all surfaces adsorb proteins and polysaccharides through molecular interactions, forming a conditioning film upon which bacteria can adhere and consume nutrients (26-30). The conditioning film has been shown to change the properties of surfaces, such as the hydrophobicity and surface charge (31, 32). These changes affect the ability of bacteria to adhere to the surface, with different bacteria attaching better to different materials and conditioning

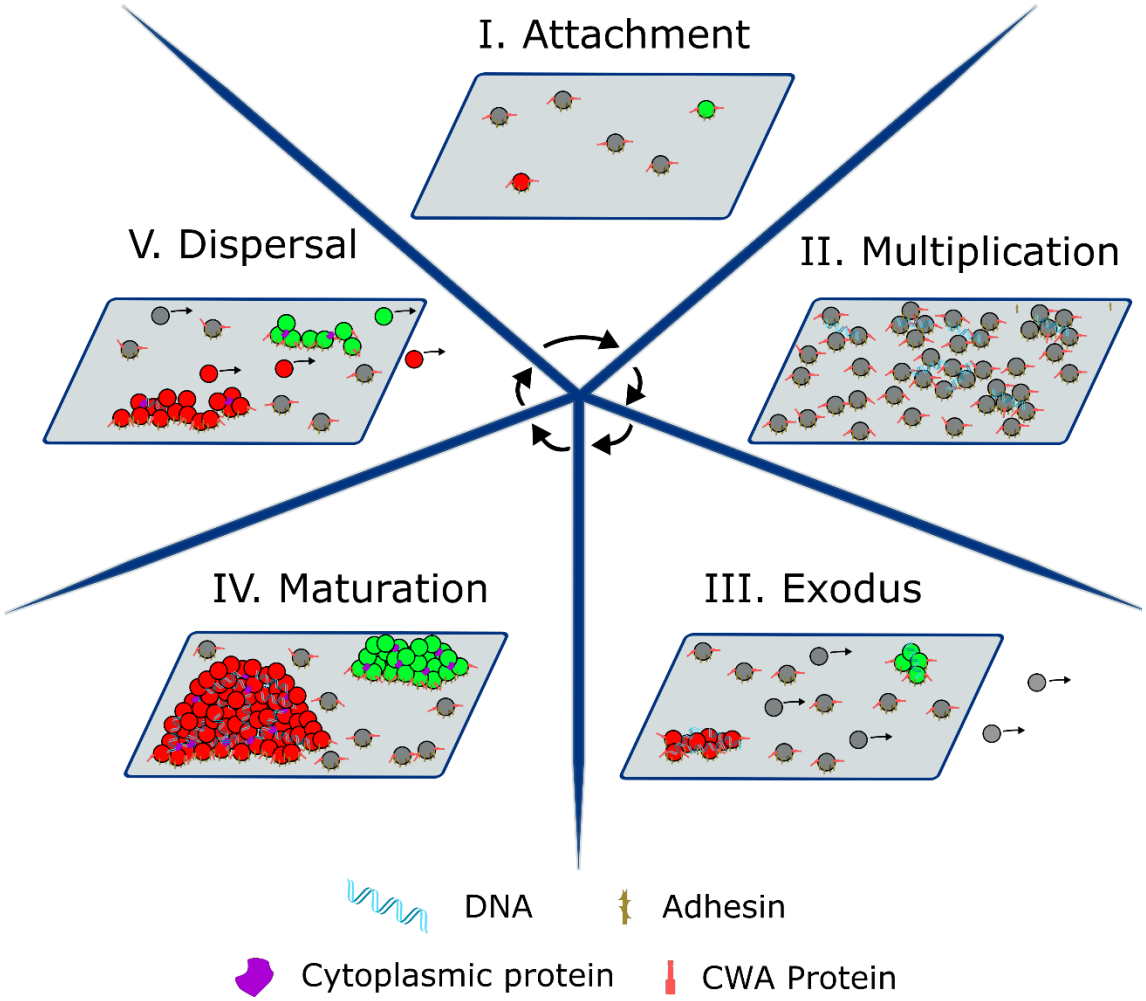

Figure 3. Heterogeneous niches arise during *S. aureus* biofilm development. *S. aureus* biofilm development occurs in five stages: attachment, multiplication, exodus, maturation, and dispersal. Various adhesins and CWA proteins are used to adhere to the surface during the attachment stage, followed by a multiplication stage where matrix components are produced and cell numbers multiply. The major matrix components are extracellular DNA and cytoplasmic proteins released from cells. Following multiplication, expression of a nuclease causes degradation of matrix eDNA, allowing a subset of the population to leave the community. This allows for the development of heterogeneous microcolonies with distinct gene expression patterns and matrix composition. Finally, quorum sensing induces expression of dispersal mechanisms that cause another subset of the population to leave the community. The dispersed cells presumably go on to form biofilms at distal sites and the cycle repeats.

films (33, 34). Importantly, this surface film can be a source of proteins and/or polysaccharides while also driving away competing organisms that may not favor the physicochemical properties of a surface/condition film.

Second, attached bacteria can remain in a favorable environment, such as near hydrothermal vents, rather than drifting away to a less suitable environment (6). As mentioned above, this may be why biofilm formation is conserved among ancient bacterial and archaeal species (35, 36), as natural selection may have favored communally driven bacteria (37).

Finally, compared to planktonic bacteria, adherent bacteria can better withstand nutrient deprivation, pH changes, immune defenses, and antimicrobial agents (4, 15-18). Adherence to a surface allows the bacteria to resist these stressors, through a variety of mechanisms. In one model, the matrix serves as a diffusion barrier to limit the penetration of molecules into the inner section of the biofilm, thus protecting the interior cells from antimicrobial agents and immune defenses (38). In another model, a subpopulation of biofilm-associated cells broadly resistant to stress (persisters) are already present prior to exposure to stress (the so-called, “bet-hedging” strategy) (39). Thus, the presence of an external stress (such as an antibiotic) results in the elimination of a large portion of the population leaving behind the persister cells, which can go on to form a new biofilm. Although other models of stress resistance exist, it is clear that the ability of bacterial cells to adhere to a surface and form a biofilm are likely to be essential for the initiation of one or more of these processes.

Adhesion requires a net attraction between the surface/conditioning film and the bacterium. Together, the van der Waals, electrostatic, and hydrophobic interactions must favor interaction for bacteria to adhere to a surface (40). Motile bacteria, like *E. coli* and

P. aeruginosa, have flagella that are used to stay near the surface as molecular interactions form with the surface (41, 42). As a non-motile bacterium, *S. aureus* (and other Gram-positive cocci) utilizes an array of proteinaceous and non-proteinaceous adhesins to strongly adhere to biotic and abiotic surfaces (43). The proteinaceous adhesins can be grouped into cell wall-anchored (CWA) proteins and non-covalently linked surface-associated proteins, whereas the non-proteinaceous adhesins consist of polysaccharide intracellular adhesin (PIA), wall teichoic acids (WTA), or lipoteichoic acid (LTA). Of the CWA proteins, the microbial surface components recognizing adhesive matrix molecules (MSCRAMMs) are the most prevalent, and consist of biofilm-associated protein (Bap) (44), clumping factor B (ClfB) (45), fibronection-binding protein A (FnBPA) and FnBPB (46, 47), *S. aureus* surface protein C (SasC) and SasG (48-50), protein A (51), and serine-aspartate repeat protein SdrC (52). These proteins contain an LPXTG motif that is recognized by sortase, which translocates these proteins across the membrane and covalently links them to peptidoglycan (53). These proteins contain ligand-binding domains for interaction with components of the host ECM, such as fibrinogen, fibronectin, and collagen (54-57). Non-covalently linked proteins involved in surface interactions are autolysin (Atl) (58-60) and secretable expanded repertoire adhesive molecules (SERAM) proteins (61). Utilizing this array of adhesins, *S. aureus* is quite successful at forming biofilms on a number of surfaces, including skin, heart valves, and catheters.

Multiplication. After attachment, biofilm cells start to proliferate and produce an ECM that is composed of polysaccharides, extracellular DNA (eDNA), and/or proteins (62, 63). The exact composition of the ECM depends on both the organism forming the biofilm and the specific signals present in the environment. In addition to its role as a structural scaffold, the ECM can retain nutrients through electrostatic interactions with

anionic fermentation products (such as formate, lactate, or acetate) and positively charged matrix components (64-66).

Like *S. epidermidis*, *S. aureus* can also produce PIA (67), but is relatively rare. However, when produced, PIA has been shown to interact with eDNA to form a scaffold for the biofilm community (68). In addition to PIA and eDNA, *S. aureus* incorporates a wide variety of proteins into the ECM (69). Like *P. aeruginosa*, many cytoplasmic proteins and virulence factors have been shown to be associated with the biofilm matrix (69). Foulston et al. and Graf et al. identified “moonlighting” cytoplasmic proteins and virulence factors that serve as electrostatic bridges between the anionic cell surface, eDNA, and metabolites (64, 65). Finally, in addition to self-produced matrix components, *S. aureus* can incorporate host matrix components, such as heparin and hyaluronic acid, into its ECM (70, 71). However, among these matrix components, eDNA is a critical component during the multiplication stage for reasons discussed in the next stage – exodus.

Exodus. Despite being non-motile, *S. aureus* biofilm formation has been observed to follow the same basic maturation and dispersal stages of development as other bacteria (72, 73). However, the characterization of *S. aureus* biofilm development with time-lapse microscopy provided important detail about the developmental process beyond what had been previously observed (25, 74). This study revealed an additional stage termed, “exodus”, that followed the initial multiplication stage (Figure 3). Exodus was shown to be induced by the expression of a secreted nuclease, which resulted in the degradation of eDNA within the biofilm matrix, allowing a subset of the cells to leave the biofilm (25). It was speculated that the exodus of these cells allows for the formation of microcolonies or “towers” during the maturation stage. Deletion of *nuc*, the gene encoding the secreted nuclease, resulted in the absence of the exodus stage, causing an uncontrolled

accumulation of cells and the lack of microcolony development. Importantly, the addition of exogenous DNase restored exodus and microcolony formation, indicating eDNA degradation is a crucial step for proper biofilm structuring during the maturation stage (25).

Maturation. The maturation stage is characterized by the emergence of 'towers' or microcolonies. During this stage, these towers display an increased growth rate, differential gene expression, and nutrient gradients as a result of the increased biomass (25, 66, 74). Heterogeneity among niches of the biofilm become evident, from matrix composition to gene expression (74). What functions these niches perform for the biofilm population is yet unclear.

Dispersal. Following maturation, degradation of the matrix or upregulation of motility allows a subset of the biofilm cells to be released and initiate biofilm development at another location. Various environmental cues can trigger dispersion, such as changes in oxygen or nutrient availability (75-80). For many organisms, including *P. aeruginosa* and *E. coli*, c-di-GMP is an important signaling molecule for dispersal and plays a major role in biofilm development (81). Environmental cues can trigger phosphodiesterases (PDEs) to hydrolyze c-di-GMP and decrease intracellular levels of the signaling molecule, causing upregulation of motility genes and repression of matrix-producing genes (82, 83). For example, *P. aeruginosa* has an oxygen-sensitive PDE, RbdA, that hydrolyzes c-di-GMP in response to low oxygen stress (76). The decrease in intracellular c-di-GMP leads to the production of rhamnolipids (a dispersant) and repression of exopolysaccharide production (76). Consistent with this finding is the observation that cells in hypoxic regions of *P. aeruginosa* biofilm structures revert to the planktonic state and disperse from the biofilm, leaving a hollowed central void (80, 84), suggesting the importance of oxygen availability for maintaining biofilm structure.

In contrast to environmental cues, dispersion can be induced by self-synthesized signaling molecules (85). For example, *S. aureus* possesses the Agr quorum sensing system that detects accumulation of a self-produced auto-inducing peptide (AIP), which can accumulate within mature biofilm structures (86). After maturation, the Agr system is activated and upregulates production of proteases and a class of peptides called phenol-soluble modulins (PSMs) that have surfactant-like properties to disrupt the matrix (73, 87). Similarly, nucleases are upregulated after maturation of structures and work to degrade matrix eDNA and help to cause cell dispersal (88).

1.1.2 Heterogeneity is an intrinsic property of bacterial communities

In recent years, heterogeneity and differential gene expression have become hallmarks of the biofilm lifestyle (66). In many ways, this was a paradigm shift given the decades of research on planktonic culture and the prevailing thought that bacterial cultures are homogeneous. These studies spawned a new way of thinking about bacterial growth and even about bacteria as complex developmental organisms. So, where does heterogeneity start? In planktonic culture prior to adherence? Upon adhesion to the surface? Or when nutrient gradients are established in the three-dimensional structure of the biofilm?

Even in planktonic culture, a clonal population can show differential gene expression patterns, whereby a subpopulation adopts a gene expression profile distinct from the rest of the population. As described by Dubnau and Losick, this heterogeneity is often controlled by what has been commonly referred to as a “bistable switch” (89). The expression of genes under the control of bistable switches can be in two alternative states, on or off, with no intermediate state. Furthermore, this bifurcation or “bistability” arises stochastically, without the influence of the environment. Bistable switches require two conditions: positive autoregulation and non-linearity. The master regulator controlling

the switch must activate its own promoter, either directly or indirectly, and require a certain threshold concentration of itself before the auto-stimulatory loop is activated (89). There is a certain amount of “noise” from the promoter of the master regulator, where there is a varying amount of expression at any given time in any given cell, stochastically giving rise to individual cells that surpass the threshold level and activates the auto-stimulatory loop (90). Bistability allows cells to “hedge bets” to be prepared for unanticipated fluctuations within the environment, such as nutrient depletion or antimicrobial exposure, by differentiating into two physiologically distinct populations. The following examples represent the documented processes known to be (or are suspected to be) under the control of a bistable switch.

Natural competence*.* Under the appropriate conditions, approximately 10% of a population of *B. subtilis* will undergo a series of regulatory events that leads to a state of “natural competence”, in which these cells produce DNA transport and recombination proteins, allowing these competent cells to import naked DNA present in the environment and incorporate it into their genomes (91, 92). In this system, ComK is the master regulator governing genetic competence. ComK auto-stimulates its own promoter in a positive feedback loop (92-94). In addition to itself, the P_{comK} promoter is affected by five other transcription factors (Rok, AbrB, CodY, DegU, and Spo0A), a protein that affects the stability of *comK* mRNA (Kre), and a quorum-sensing system (MecA and ComS) (95-105). Clearly, the cell has placed numerous safeguards to tightly modulate competency, since the physiology of the cell is greatly affected by blocking growth, cell division, and DNA replication (106, 107). A theoretical analysis by Kussell and Leibler suggests bistability is the optimal strategy for coping with infrequent changes in the environment because a subpopulation is already adapted to the new environment, thus ensuring survival of the clonal population (108). In the case of *B. subtilis* competence,

diverting 10% of the population towards natural competence strikes a balance between optimal growth for most of the population while maintaining a reserve of cells adapted to respond to potential challenges.

Virulence factor expression. Another example of bistability is the SaePQRS multicomponent regulatory system in *S. aureus*, which regulates the expression of various virulence factors, including the staphylococcal thermonuclease encoded by *nuc*. Prior to the exodus stage of *S. aureus* biofilm development, a stochastic bifurcation results in the formation of two cell populations that differentially express *nuc*, a target of the SaePQRS regulatory system that degrades eDNA within the matrix of the biofilm and induces the exodus stage (25). In a study by DelMain et al., other targets of the SaePQRS system (*coa* and *selX*) were shown to be under stochastic control (109). Furthermore, strains with constitutively activated SaeS abrogated stochastic expression, demonstrating expression of SaePQRS targets in all cells, suggesting this regulator may function as a bistable switch. Although the SaePQRS-mediated bistable control of gene expression was first observed during biofilm development, bistable expression is not limited to biofilm conditions. DelMain et al. showed that the expression of *nuc* is also stochastic in planktonic conditions and was likewise dependent on SaeS, mirroring the gene expression observations of *S. aureus* biofilms (109).

Surface contact. Upon contact with a surface, *P. aeruginosa* and *E. coli* utilize c-di-GMP-mediated signal transduction pathways to communicate a transition to sessility (110, 111). A recent study by Armbruster et al. showed that the c-di-GMP signal transduction upon *P. aeruginosa* contact with the surface is not uniform, and marked heterogeneity arises among the population (112). They discovered that the Wsp regulatory system, which localizes laterally along the cell and senses contact with surfaces, generates two physiologically distinct subpopulations through heterogeneous

c-di-GMP signaling. One subpopulation has high amounts of c-di-GMP and produces polysaccharides required for biofilm formation, whereas the other subpopulation has low amounts of c-di-GMP and explores the surface through Type IV pili ((112), Figure 4). Both subpopulations are required for efficient biofilm formation, representing a good example of division of labor during early biofilm formation.

Matrix production. Another recent study in *E. coli* revealed that local matrix heterogeneity in macrocolony biofilm formation is controlled by a c-di-GMP-dependent bistable switch. However, in this case, the c-di-GMP-mediated heterogeneity is controlled by several nested positive and negative feedback loops (113). In this switch, c-di-GMP levels are intricately controlled by several phosphodiesterases (PdeR and PdeH) and diguanylate cycles (DgcM and DgcE). PdeR and DgcM interact with each other and the MlrA transcription factor, the intermediate level regulator of the σ^S/MlrA/CsgD transcription factor cascade that controls curli fiber and cellulose synthesis (114-119). PdeH and DgcE are antagonistically acting enzymes that control c-di-GMP input into the PdhR/DgcM module, particularly as cells approach stationary phase (115, 116, 119). *pdeH* is upregulated by σ^S, a transcriptional regulator active during stationary phase, whereas *dgcE* is upregulated by σ^{FliA}, a transcriptional regulator that modulates expression of genes involved in motility and flagellar biosynthesis (115, 120). When c-di-GMP from the PdeH/DgcE module is present, like during the transition to stationary phase, PdhR dissociates from a direct interaction with DgcM to degrade the c-di-GMP generated from the PdeH/DgcE module. Then, since PdhR is no longer associated, the diguanylate cyclase activity of DgcM is activated. Furthermore, DgcM can interact with MlrA and activate expression of *csgD*, the transcriptional regulator responsible for activation of curli fiber and cellulose production (116).

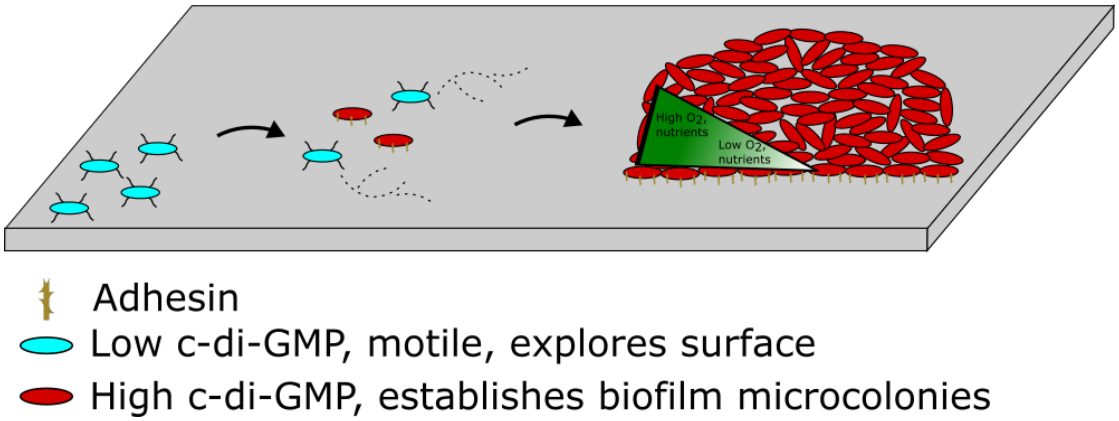

Figure 4 Contact with the surface generates a heterogeneous response that leads to biofilm formation. When *P. aeruginosa* comes into contact with a surface, a laterally localized Wsp regulatory system senses the contact and generates two distinct populations: one with high amounts of c-di-GMP and one with low amounts of c-di-GMP. The population with low c-di-GMP continues to explore the surface whereas the population with high c-di-GMP downregulates motility and upregulates production of matrix components. Following the development of microcolonies, gradients of nutrients and oxygen are established, and cells respond to their own microenvironment accordingly. For example, hypoxia-induced genes are upregulated within the center of the microcolony.

In the “intermediate macrocolony zone”, where matrix-free and matrix-producing cells are adjacent to each other, Serra and Hengge found that the PdeR/DgcM switch modulates the local matrix heterogeneity found within this zone (113). Furthermore, the heterogeneity is not a biofilm-specific behavior, as planktonic cells also differentiated into matrix-producing and matrix-free subpopulations upon entry into stationary phase, when cells begin to express *csgD*.

In subsequent studies, the long-range vertical asymmetry of the matrix architecture within macrocolony biofilms was found to be due to differential expression of PdeH and DgcE (115, 116, 119). In wild-type biofilms, the upper layer features a homogeneous “dense brickwork” matrix composed of cellulose and curli fibers (118, 121, 122). A double-knockout of *pdeH* and *dgcE* abrogated the “dense brickwork” matrix and the upper layer resembled the architecture found in the heterogeneous horizontal network in the lower part of the intermediate macrocolony zone (113). Thus, the vertically asymmetrical matrix architecture that is characteristic of *E. coli* macrocolony biofilms was eliminated, showing the importance of PdeH/DgcE input into the PdeR/DgcM switch. Interestingly, *pdeH* expression in macrocolonies follows a vertical nutrient gradient, with high expression in the bottom layer and decreasingly lower expression further up the macrocolony structure (118), indicating nutrient gradients play a role in the structuring and heterogeneity of *E. coli* macrocolony matrix production.

A recent study of *B. subtilis* biofilms found a division of labor in the production of the two biofilm matrix components, TasA and EPS (19). Using a fluorescent gene reporter approach, the differentiation of the cells into three phenotypic populations was observed: EPS producers, non-producers, and “generalists” that produced both TasA and EPS. As is a common feature among biofilms, these differentiated subpopulations were stratified into spatially distinct niches within the biofilm (19, 74). Specialization allows for the

population to minimize the metabolic costs to produce biofilm matrix molecules, thus, supporting optimal biofilm expansion and growth (19), a common theme among the examples of biofilm heterogeneity given in this chapter.

Though the ECM is often thought to be a passive structural scaffold that holds together biofilm bacteria, it also exerts profound effects on the biofilm cells. For instance, the TasA amyloid protein produced by *B. subtilis* can be toxic to vegetative cells (123). However, due to the heterogeneous distribution of TasA, only vegetative cells near TasA-producers are affected. The ECM also affects gene expression, as seen by multiple examples of bacteria sensing an ECM component and transducing that signal into a response that furthers the development of the biofilm. For example, *P. aeruginosa* biofilm cells detect the presence of Psl and uses it as a signal to promote additional ECM production, helping build the matrix during the early stages of biofilm development (124). In another example of a positive feedback loop that increases ECM production, the *epsA-O* operon in *B. subtilis* not only encodes enzymes involved in the production of EPS, but also an EPS-sensing membrane protein coupled with a tyrosine kinase. In the presence of EPS, these proteins transduce a signal to increase expression of the *epsA-O* operon in a positive feedback loop (125). In *S. aureus*, DNA-binding proteins form an electrostatic net with eDNA. A recent study showed that overexpression of one of these proteins, a lipoprotein named SaeP, increased biofilm formation capacity and expression of *nuc*. Since this lipoprotein is an auxiliary component of the SaeRS two-component system (TCS), SaeP may have a regulatory role in addition to its role in the electrostatic net of the ECM (126).

Metabolism. In patients with dental caries, polymicrobial communities on the tooth surface are precisely arranged in a corona-like architecture mediated by an extracellular scaffold produced by *Streptococcus mutans* that positions other oral microbes and

creates localized regions of acidic pH (127). In *P. aeruginosa*, the three-dimensional architecture of biofilms has been shown to foster the development of chemical and nutrient gradients, where nutrients are readily available for peripheral cells but limited for the inner cells of the biofilm (66, 128). These chemical and nutrient gradients establish microenvironments that follow the gradient pattern. Using laser capture microscopy, Williamson et al. isolated fractions of *P. aeruginosa* biofilms and found gradients of mRNA abundance, growth rates, and antibiotic tolerance (129). As expected, cells on the periphery of the *P. aeruginosa* biofilms were metabolically active, had higher mRNA levels, and were actively dividing. However, the cells at the bottom of the biofilm grew slower, had little expression of housekeeping metabolic genes, and were more tolerant to antibiotics that target actively dividing cells (129). When gradients of nutrients and oxygen are established within mature biofilm structures, the cells utilize a variety of sensory strategies to alter gene expression. For example, *E. coli* utilizes approximately 30 TCSs to respond to environmental signals such as pH, osmolarity, and oxygen (130). The signals transduced from the environment impact metabolism, virulence factor production, and gene expression (118, 131-133).

In *S. aureus* biofilms, genes induced by hypoxic conditions, *ldh1* and *cidABC*, were upregulated within the center of large towers of *S. aureus* biofilms, indicating there is an oxygen gradient in *S. aureus* biofilm microcolonies like the oxygen gradients seen in *P. aeruginosa* biofilms (74, 134, 135). Similarly, hypoxic cytochromes are more highly expressed in the internal regions of mature *E. coli* biofilms as a result of the more limited oxygen levels within these regions of the biofilm (132).

Although the varied extracellular signals within a biofilm clearly have local impacts on cellular physiology and gene expression in *S. aureus*, other aspects of the differential expression of the *cidABC* and *lrgAB* operons, both involved in bacterial programmed cell

death (PCD), cannot be attributed to differences in microenvironment alone. For example, there are three distinct niches we can identify in *S. aureus* biofilms grown in microfluidic flow conditions: fast-growing large microcolonies that express *lrgAB* and *cidABC*, slower-growing small microcolonies that express *cidABC* only, and a basal layer that coats the surface and expresses neither *cidABC* and *lrgAB*. Both operons are controlled by regulators, CidR and LytSR, that are responsive to different metabolic cues (136-139), suggesting that these microcolony types represent different metabolic states. Furthermore, the two different microcolony types also exhibit differential staining for eDNA, with the large microcolonies containing eDNA within their matrices, whereas the small microcolonies do not. Since differential *cidABC* and *lrgAB* expression occurs prior to the formation of mature biofilm structures, these observations suggest that metabolic heterogeneity arises before the microcolonies form, possibly representing another form of bistability (74).

Persister formation. Biofilms are notoriously tolerant to antibiotic treatment, of which persistence plays a key role. Persistence occurs when a subpopulation of cells is tolerant to antibiotics, either through mutation or slow growth. It is most easily observed after the treatment of cells with antibiotic and the generation of a bimodal time-kill curve where the majority of the population is killed but a subpopulation remains (140). These persister cells, or persisters, can withstand the killing effects of antibiotics but can not grow in their presence (141, 142). Once antibiotic pressure is relieved, persisters can resume normal growth and are still susceptible to antibiotics (142, 143). To survive the antibiotic pressure without a resistance mechanism to break down, export, or modify the antibiotic or its target (144), persisters adopt a dormant state that down regulates cellular processes targeted by antibiotics (145-147). All bacterial populations are thought to contain a small subpopulation of persisters (148, 149) and the frequency of persister cell

formation is highest in stationary phase culture and during the biofilm mode of growth (39, 146, 150).

One major mechanism to enter and maintain the dormant state is through paired toxin-antitoxin (TA) systems (39, 151-154). TA systems are typically comprised of a stable protein toxin, which can shut down cellular processes, and an unstable antitoxin that inhibits the toxin and is typically an mRNA or protein (155, 156). The most famous example of a TA pair is HipAB, the first to be identified and tied to persister cell formation (157-159). In this system, HipA is a toxin that blocks translation by phosphorylating glutamyl-tRNA-synthetase, leading to a buildup of uncharged $tRNA^{Glu}$ and synthesis of the stress response molecule ppGpp (160-162). HipB is the antitoxin of the pair and directly interacts with HipA, causing a conformational change that inhibits the activity of HipA (158, 163, 164). A gain-of-function mutation in *hipA*, named *hipA7*, enhanced persistence up to 1,000-fold (157). Analyses of the HipBA promoter complexes showed that HipA forms homodimers in complexes with HipB and auto-represses its own expression (165). The *hipA7* mutation is located at the HipA-HipA homodimer interface and caused lower affinity between HipA and HipB, resulting in higher levels of free HipA that is more stable than the free HipB (165). Thus, several feedback loops that can explain bistability of the HipAB TA system have been proposed that depend upon HipB instability, dilution effects from cellular division, and involvement of the stringent response and proteolytic degradation of HipB (154, 166-170). Overall, the involvement of ppGpp and the stress response is a common theme among TA systems (171, 172). Through this stress response system, stress signals such as amino acid depletion or nutrient limitation (173, 174) disrupt the direct binding of antitoxins to their cognate toxin pair (171) and cause persistence.

In addition to environmental factors, bistability and stochastic gene expression play an important role in the activation of persistence mechanisms (175). For example, Rotem et al. (176) found that the HipAB TA system is controlled by a bistable switch by showing there is a threshold concentration of HipA required for persistence and the duration of persistence depended on how far the threshold was exceeded. In addition to HipAB, stochastic and non-genetic variability, such as membrane permeability, growth rates, efflux pumps and porins, cell division events, govern persistence mechanisms (177-179). As we learn more about mechanisms of persistence, there is continued appreciation for the different ways persister cells are generated and the potential bistable switches that control their formation.

1.2 CodY and CcpA regulate central metabolism and help coordinate biofilm development

S. aureus is adaptable to many environments, as evidenced by the plethora of sites it can infect in the human body (180). This adaptability can be attributed to the metabolic versatility available to the organism and its ability to overhaul the regulatory networks governing metabolism and virulence (181, 182). Two major regulators of staphylococcal metabolism are CodY and CcpA.

CodY. CodY is a global regulator in Gram positive bacteria, directly or indirectly regulating over 200 genes, including many metabolic and virulence genes (183). CodY activity is regulated by levels of branched chain amino acids (BCAAs) and GTP, with isoleucine predominantly regulating CodY activity (184). Under nutrient rich conditions, *S. aureus* scavenges BCAAs from the environment rather than utilize BCAA biosynthetic pathways (185). As nutrients become depleted from the environment and levels of BCAAs and GTP decrease, CodY loses affinity for its targets in an order that depends

on how closely the target gene's CodY binding site matches the consensus sequence (183, 186). Oddly enough, genes with similar CodY binding affinity can be grouped by their function. For example, nutrient transporters are derepressed first, followed by metabolic synthesis pathways, then virulence factors used to damage tissue and scavenge resources (186). This stepwise regulation allows *S. aureus* to adapt to a wide variety of environments.

Studies have produced mixed results on the effect of CodY inactivation on biofilm formation, as some studies showed increased biomass in a *codY* mutant whereas others showed decreased biomass in a *codY* mutant (187, 188). Atwood *et al.* showed this observation could be due to the strain's ability to produce PIA, which is correlated with methicillin resistance (189). *codY* appears to decrease biomass in methicillin-resistant strains, which typically have little PIA production. In PIA-producing strains, which are typically methicillin-susceptible, a *codY* mutant biofilm appears very "stringy" with structures tethered together by eDNA and PIA (68). The *codY* mutant overproduces PIA in these strain backgrounds because CodY represses the gene operon encoding PIA biosynthesis pathway, *icaADBC*. As a result, the mutant overproduces this positively charged matrix polysaccharide, which in turn acts as a sponge for negatively charged eDNA.

CcpA. *S. aureus* undergoes carbon catabolite repression (CCR) to consume preferred carbon sources before turning on pathways involved in utilizing secondary carbon sources, such as amino acids. Carbon catabolite protein A (CcpA) is a global regulator that mediates CCR and carbon catabolite activation (CCA) in *S. aureus* (190, 191). To achieve this purpose, CcpA works with a phosphotransferase (Hpr), a bifunctional kinase/phosphatase (HprK), and a sugar phosphotransferase system (PTS) (191). CcpA controls two regulons, determined by dependency on glucose. However,

most CcpA-regulated genes are glucose-dependent (192). CcpA can form complexes with several partners, including HPr and CodY (193). When glucose enters the cells through PTS, HPr is phosphorylated at a serine residue, after which it can form a complex with CcpA. The CcpA-HPr-Ser46-P complex has increased affinity for *cis*-acting DNA sequences called catabolite responsive element (*cre*) sites (190), which is further enhanced by increasing levels of fructose-1,6-bisphosphate (194). CcpA represses genes within the TCA cycle and secondary carbon source catabolism, such as amino acids, while activating the glycolytic and fermentative pathways (195). Inactivation of CcpA results in a loss of biofilm biomass, though *ccpA* mutants still adhere to surfaces (196, 197).

Interplay of metabolic regulators and effect on virulence. During an infection, the host will attempt to sequester nutrients and resources from the invading pathogen. As nutrients become scarce, *S. aureus* upregulates expression of virulence factors that aid acquisition of nutrients from the host, such as toxins that lyse surrounding host cells. As mentioned above, CcpA and CodY each respond to environmental signals, through levels of FBP and BCAAs/GTP, respectively, and connect at key nodes of central metabolism (190, 192, 198). Together, these two regulators sense the nutritional environment and govern flow of carbon and nitrogen by controlling catabolic and anabolic pathways involved in sugar and amino acid utilization. As such, it's no surprise that these regulators influence the expression of these virulence factor and nutrient acquisition genes, too. For example, CodY represses the expression of toxins such as alpha-toxin and nuclease (185). On the other hand, CcpA represses the expression of alpha-toxin, capsule, and protein A (199). Under nutrient limitation, the expression of these regulatory targets is derepressed, allowing *S. aureus* to target and acquire nutrients from the host.

2 Materials and Methods

Table 1. List of strains used in this study.

Bacterial Strains	**Description**	**Reference**
Escherichia coli		
DH5α	Strain used to construct recombinant plasmids	(200)
S. aureus		
RN4220	Restriction-deficient strain, highly transformable	(201)
UAMS-1		(202)
UAMS-1 *codY::erm*	UAMS-1 *codY::erm*	(187)
UAMS-1 *ccpA::tet*	UAMS-1 *ccpA::tet*	(203)
UAMS-1 *codY::erm ccpA::tet*	UAMS-1 *codY::erm ccpA::tet*	This study
Plasmids		
pMRSII	Cloning vector	(109)
pLB1	*ackA* promoter::sGFP, Cm^R	This study
pLB18	*pfkA* promoter::sGFP, Cm^R	This study
pLB19	*pfkA* promoter::sGFP, *cidABC* promoter::sDsRed, Cm^R	This study
pLB22	*citZ* promoter::sGFP, *cidABC* promoter::sDsRed, Cm^R	This study

Table 2. Oligonucleotides used in this study

Primer name	Sequence
pLB1-BamHI-ackA-r	5'-GCCGGGATCCATCGTTTGCTTTTTATACTATTTCATTTTCATTTTATC-3'
pLB1-SphI-ackA-f	5'-CGGCGCATGCCGAAGAAGGACATAGTTATTCACA-3'
GFP-KpnI-pfkA-f	5'-GCCGGTACCGCTGAAACAATGAAAATTACTGC-3'
GFP-EcoRI-pfkA-r	5'-CGCGAATTCCTGATTTATCTTTAACTCTAAATTACCAC-3'
GFP-KpnI-citZ-f	5'-GCCGGTACCCGGTAAAAATGTGTAAAATTCCATG-3'
GFP-EcoRI-citZ-r	5'-CGCGAATTCCCTTTACTGTTTCTTTATGAAATGG-3'
dsRed-NheI-cidABC-f	5'-GCGGCTAGCGGAACGCTTGAATGGACTGGAAAC-3'
dsRed-BamHI-cidABC-r2	5'-GCCGGATCCTAAATACGTCTAAATTGTTACAATAACTATTATAAAGATGGCG-3'
SAV1737-f	5'- GCAACAAAGGACCATTTAACGATAATAC -3'
acuC-f	5'- GGTGGACTTGAAATATTCGCTACAG -3'
cna-f	5'- AGTGACATGGTCTAATCTTCCGG -3'
cna-r	5'- TCCACTTTTGATGGCTTATCTGG -3'
RT-rpoD-f	5'- AACTGAATCCAAGTGATCTTAGTGCC -3'
RT-rpoD-r	5'- TCATCACCTTGTTCAATACGTTTGG -3'
RT-alsS-f	5'- GAAGTCACTATATTTGGATGGCACG -3'
RT-alsS-r	5'- CAACTTGCGTATTAGGGCGTAC -3'
RT-pfkA-f	5'- GCAGTTGTTCGTACAGCAATTTACAATG -3'
RT-pfkA-r2	5'- GAATGTACCTCCACGCTGAATCG -3'
RT-glmU-f	5'- CGATAATTTTGGCAGCAGGTAAAGG -3'
RT-glmU-r	5'- GATCGACACCAGAGCCTTTCAC -3'
RT-icaA-f	5'- CTCAATCAAGGCATTAAACAGGCTTC -3'
RT-icaA-r	5'- CCTGTAACTGCACCAAGTTTTGG -3'
RT-citZ-f	5'- CAGATCACGTGCATCCAATGAC -3'
RT-citZ-r	5'- CTCGAGCAAACGCTGTAACTAATG -3'
RT-ackA-f	5'- GTTTCAATTAATCAGAATGCCTGAAGAGG -3'
RT-ackA-r	5'- GCTTCAACATGATCCTTGATATCTTGTACTG -3'
RT-pta-f	5'- CGTATTACCTGAAGGAGAGGACG -3'
RT-pta-r	5'- GCTTTCAATTCACTTGTCGCAGG -3'
RT-ldh1-f	5'- GGTAATGGTGCAGTAGGTTCAATC -3'
RT-ldh1-r	5'- CTGTTGTTGGAGAATATGGTGTGG -3'
RT-accD-f	5'- CCTGCAGGTATTATGACTAAGTGTCC -3'
RT-accD-r	5'- GCTTCTATACGTTTATACGCAGTTAAAGCA -3'
RT-pyc-f	5'- GCTCGTACAACGGCTATCAAG -3'
RT-pyc-r	5'- CATTAGCGGGAAACCAGCTTC -3'
RT-ilvD-f	5'- GCTAAAGAAGCAATTAGAGAAGCCG -3'
RT-ilvD-r	5'- TCACGTGATGGTAGAGAATATCGC -3'
RT-pgi-f	5'- TGGTGCAGGTAGTGACTTCTTAG -3'

RT-pgi-r	5’- AGAACCACCAATACCGATGACTAC -3’
RT-pdhA-f	5’- AGTTACAAGCCCAATTCGATGC -3’
RT-pdhA-r	5’- TTGTTCATCCGTAAGATCAGGTACTAAG -3’
RT-cidA-f	5’- GCACAAAGTCCAATTAATAATCAAATTATTACTACAAC -3’
RT-cidA-r	5’- GTAAATAAAATAAAAATAGACCAACAATACTGCCG -3’

2.1 Bacterial strains and culturing

All strains used in this study are listed in Table 1 in the supplemental material. Staphylococcus aureus strains were cultured in tryptic soy broth (TSB) (Becton Dickinson formulation without dextrose) supplemented with 0.25% [wt/vol] glucose at 37°C with shaking at 250 rpm, unless otherwise specified. *E. coli* strains were cultured in Luria-Bertani (LB) broth. When necessary, antibiotics were added to media during strain construction and selection [chloramphenicol (10 µg ml-1) (Fisher Scientific), erythromycin (5 µg ml-1) (TCI America), tetracycline (5 µg ml-1) (Fisher Scientific), ampicillin (100 µg ml-1) (Sigma)]. Metabolite and RNA-seq analyses were performed after three hours or six hours of growth, unless otherwise noted.

The UAMS-1-*codY ccpA* double mutant was generated by bacteriophage Φ11-mediated transduction (204) of the *ccpA::tetL* allele from the JE2 *ccpA::tetL* strain (205) into UAMS-1-*codY::ermC* (187). The replacement of the *ccpA* gene by the *ccpA::tetL* allele was verified by PCR using primers SAV1737-f and acuC-f (203). The UAMS-1 background in all mutants was confirmed by PCR using primers cna-f and cna-r (206).

2.2 Bioflux1000, gene expression analysis, and matrix degradation treatments

S. aureus biofilm development was assessed using a BioFlux 1000 microfluidic system (Fluxion Biosciences, Inc., San Francisco, CA), as previously described (74). Briefly, to grow biofilms in the BioFlux system, the channels in a 48-well plate were first primed with 210 µl of TSB for one minute at 20.0 dynes/cm^2. After priming the channels, 300 µl of fresh 50% TSB supplemented with 0.125% glucose was added to the input wells and 210 µl of inoculant containing exponentially growing cells diluted to an OD_{600} of 0.8 was added to the output wells. The channels were seeded by pumping from the

output wells to the input wells at 2.0 dynes/cm^2 for 3 - 6 seconds. After allowing cells to attach for one hour at 37°C, excess inoculant was aspirated from the output well, and 1.0 ml of 50% TSB supplemented with 0.125% glucose was added to the input well and pumped at 0.6 dyne/cm2 for 18 h (flow rate, 64 µl/h). After six hours of biofilm formation in the flow cell, fresh media in the inlet wells were replaced with fresh media alone or fresh media containing matrix-disrupting enzymes or chemicals with treatments [DNase I (10 U ml-1), Proteinase K (100 mg ul-1), or sodium metaperiodate (2 mM)]. Bright-field and fluorescent images were taken every five minutes at 200×magnification. The settings for gain and exposure were kept constant for all images, of which representative images are shown for each time point and strain.

2.3 Construction of reporter plasmids

Promoters for *pfkA*, *citZ*, and *ackA* were PCR-amplified using primers listed in Table 2 and PrimeSTAR HS DNA Polymerase (Takara Bio) using the manufacturer's instructions. For pLB1, the *ackA* promoter PCR product and pMRSII vector were digested with BamHI and SphI restriction endonucleases. Then, these fragments were ligated using Blunt/TA Ligase Master Mix (New England Biolabs) and successful cloning was confirmed by nucleotide sequencing. Dual reporters were constructed by first placing the *pfkA* promoter in front of *sgfp* in pMRSII, by digesting the *pfkA* promoter PCR product and pMRSII vector with KpnI and EcoRI then ligating the fragments using Blunt/TA Ligase Master Mix (New England Biolabs), making pLB18. Next, pLB18 and the *cidABC* promoter PCR product were digested with NheI and BamHI, followed by ligation to complete the construction of the pLB19 dual *pfkA::sgfp cidABC::sDsRed* reporter. Finally, pLB22 was constructed by excising the *pfkA* promoter from pLB19 by digesting with KpnI and EcoRI, gel purifying the band containing the vector with *cidABC::sDsRed*, then ligated to the KpnI- and EcoRI-digested *citZ* promoter fragment.

2.4 Metabolite analyses

2.4.1 Lactate, acetate, glucose, ammonia kits

Samples for metabolite analyses were prepared by centrifuging one ml aliquots of bacterial cultures for 3 min at 14,000 rpm at 4°C. The supernatants were removed and stored at −20°C until use. Acetate, glucose, and ammonia concentrations were determined using kits purchased from R-Biopharm, according to the manufacturer's protocol.

2.4.2 Acetoin assay

Acetoin concentrations were determined at 560 nm as described previously (207). Briefly, 140 µl of creatine (0.5% [wt/vol] in water), 200 µl of α-naphthol (5% [wt/vol] in 95% ethanol), and 200 µl KOH (40% [wt/vol] in water) were added in that order to 200 µl of acetoin standard solution or diluted culture supernatant, with mixing after each reagent was added. Then, samples were incubated for 15 minutes at room temperature before mixing again, immediately followed by measurement of absorbance at 560 nm in the spectrophotometer. The assay was linear over the entire absorbance range of the spectrophotometer.

2.4.3 HPLC analysis of biofilm effluent

Biofilms were grown in a Bioflux1000 instrument and effluent was collected every 2 hours by extracting excess media from the outlet wells. Since bacteria can reside in the outlet wells and produce waste, we removed all media from the outlet wells 0.5 h prior to collection time points. The effluent that accumulated for a half hour was collected, centrifuged for 3 minutes, and the supernatant was frozen at -20°C until use. Due to small sample volumes, effluents from 8 wells were pooled together for a single replicate (of 3 replicates measured) and measured using High-Performance Liquid

Chromatography as previously described (208). Briefly, a 0.2-µm-pore-size nylon filter was used to filter the supernatants, which were then put through a Bio-Rad Aminex HPX-87 column (Bio-Rad) to separate the metabolites. An autosampler injected 5 µl of sample volume into a thermostatically controlled column (maintained at 65°C), where analytes were eluted isocratically with 0.005 M H_2SO_4 at 0.5 ml/min for 30 min. Chromatograms were integrated using Agilent ChemStation analysis software.

2.5 Metabolomics

Samples were prepared as previously described for metabolomics analysis (209). Briefly, strains were inoculated in TSB supplemented with 0.25% glucose to an OD_{600} of 0.05 and grown aerobically at 37°C with shaking at 250 rpm. 10 optical units of bacterial cultures were harvested and filtered through 0.45 µm membrane (Millipore). Two washes of five ml cold saline were performed on the membrane-trapped cells, followed by quenching in ice-cold 60% ethanol containing 2 µM Br-ATP as an internal control. Next, cells were lysed with a bead homogenizer set to oscillate for three cycles (30 s) of 6,800 rpm with a 10-s pause between each cycle. The tubes were centrifuged at 13,000 rpm and the supernatant was collected, lyophilized, and stored at −80°C.

2.6 mRNA quantification using RT-PCR

RNA was isolated from *S. aureus* cultures after 3 h and 6 h of growth in TSB supplemented with 0.25% glucose as described previously (210). Gene-specific primers (*rpoD*, *pfkA*, *citZ*, *icaA*, *pta*, *ackA*, *pdhA*, *pgi*, *alsS*, *cidA*, *glmU*, *ldh1*, *pyc*, *ilvD*, and *accD*) were used to perform quantitative real-time PCR (Table S1). Briefly, 1 µg of total RNA was used to synthesize cDNA using the QuantiNova Reverse Transcription Kit (Qiagen). cDNA products were amplified from a 1:10 dilution of the samples using the LightCycler FastStart DNA Master SYBR green I kit (Roche Applied Science) following the

manufacturer's protocol. Results reflect 3 biological replicates of each sample measured in duplicate. The comparative threshold cycle (CT) method (211) was used to calculate the relative transcript levels with normalization to *rpoD* transcripts.

2.7 RNA-seq

S. aureus mRNA was sequenced using a NextSeq 550 System with Mid-Output to acquire 150 single base pair reads. Assembly and analysis were performed using CLC Genomics software.

2.8 PIA immunoblot

PIA accumulation was determined as previously described (210). Briefly, TSB medium containing 0.25% glucose was inoculated with equal numbers of bacteria from overnight cultures. The cultures were grown for 3 h at 37°C with a flask-to-medium ratio of 10:1 and aerated at 250 rpm. Equal numbers of bacteria were harvested by centrifugation (2.0 OD_{600} units), and the PIA was extracted in 0.5 M EDTA by boiling for 10 min and freezing overnight. Samples were incubated with proteinase K for 1 h at 37°C, followed by boiling for 5 min to inactivate proteinase K. Aliquots of PIA were applied to a neutral nylon membrane (GVS North America) and blocked with 5% skim milk for 6 h. The nylon membrane was incubated overnight with PIA-specific antibodies, followed by a 4-h incubation with an anti-rabbit immunoglobulin G–peroxidase conjugate. The presence of PIA was detected using SuperSignal West Pico chemiluminescent substrate (Pierce).

3 Metabolic heterogeneity gives rise to diverse microcolonies with differences in gene expression and matrix composition

Heterogeneity is a seemingly embedded feature of life (66). It can muddy the waters of data analysis, as we tend to try to characterize the most common behavior of a population and make conclusions based on our understanding of that behavior. Our understanding of how physiological heterogeneity arises in bacteria is limited, as not a lot of focus has been placed on this phenomenon. In biofilms, many studies have pointed to chemical and nutrient gradients causing heterogeneous niches to form (66, 129, 212). However, recent studies have shown heterogeneity starts upon contact with a surface, far sooner than the formation of nutrient gradients (112).

In our laboratory, we have endeavored to characterize biofilm development using a microfluidic flow cell system called the Bioflux1000. Early into our observations, we discovered differential gene expression between different niches of the biofilm that developed after the exodus stage (74). These niches consisted of a basal layer, a small tower type, and a large tower type. The basal layer did not grow as fast as the cells in either of the towers, whereas the large tower cells grew the fastest. We characterized the two tower types based on their expression of two operons (*cidABC* and *lrgAB*) and incorporation of dead cells and eDNA into these towers. The small towers constitutively expressed *cidABC* whereas the large tower only expressed *cidABC* after a substantial biomass had been achieved. Furthermore, the large tower was the only niche that expressed *lrgAB*, which it did constitutively. The expression of *cidABC* and *lrgAB* began for these towers from the onset of their growth, indicating the nutritional environment had little to do with triggering their development as there is a constant flow of nutrients in this

system. Does heterogeneity arise stochastically, a response to localized nutrient gradients, or perhaps both?

In this chapter, we will discuss the heterogenic nature of *S. aureus* biofilm development, particularly as it pertains to metabolic shifts within subpopulations of the biofilm during the maturation stage of development.

3.1 Metabolite analysis reveals existence of multiple biofilm niches in a constant flow environment

After the exodus stage of *S. aureus* biofilm development, subpopulations of cells undergo rapid growth, differential expression of *cidABC* and *lrgAB*, with the ultimate formation of morphologically diverse microcolonies (74). Since the regulators for *cidABC* and *lrgAB* respond to metabolic cues, we hypothesized there is a stochastic change in the expression of metabolic genes that leads to the development of diverse biofilm niches.

S. aureus is an organism with a preferred carbon source: glucose (191). When in the presence of excess oxygen and glucose, *S. aureus* will rapidly consume glucose, produce and secrete acetate, and regenerate reducing equivalents through the respiratory chain (Figure 5A). Once glucose is fully consumed, *S. aureus* will consume acetate to fuel the TCA cycle and continue aerobic respiration (213, 214). When oxygen is limited, as in a hypoxic environment, *S. aureus* will rapidly consume glucose but instead of producing acetate it produces lactate, due to a drop in respiratory chain activity and a need to regenerate NAD^+ to support glycolytic activity (Figure 5B) (213, 215). To investigate the establishment of niches during *S. aureus* biofilm development, we measured the metabolic byproducts of biofilms grown in a microfluidic flow cell

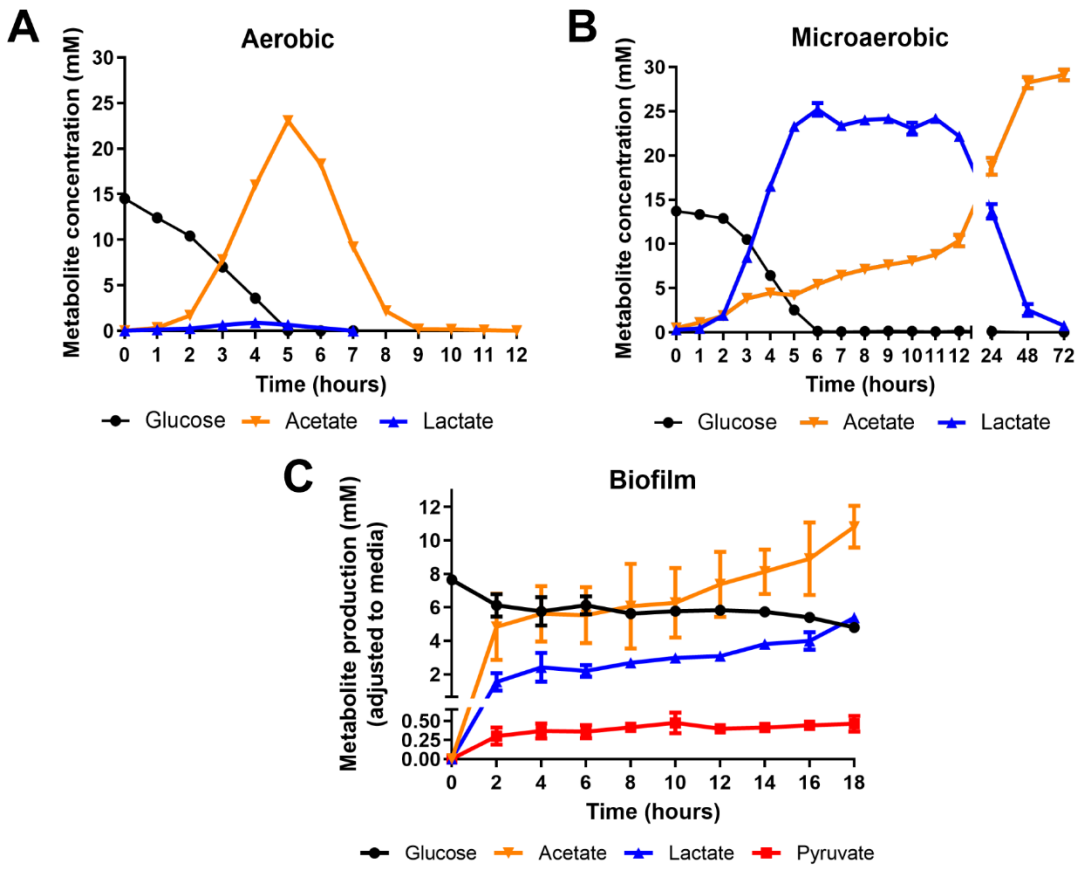

Figure 5. Characterization of metabolites produced in aerobic, microaerobic, and biofilm conditions. (A) In aerobic conditions, glucose is rapidly consumed and used to produce acetate. After exhaustion of glucose, acetate is used as a carbon source to support further growth. (B) In microaerobic conditions, reduced respiratory chain activity requires cells to utilize *ldh1* to produce lactate while regenerating NAD^+ to support glycolytic activity. Meanwhile, acetate production remains active but at a much lower level than in aerobic conditions. (C) Biofilms grown in a constant flow environment produce acetate, lactate, and pyruvate as metabolic byproducts, indicating the presence of multiple metabolic niches.

system by collecting samples every two hours. We observed the formation of multiple metabolic niches by the very first timepoint measured, as indicated by robust production of both acetate and lactate (Figure 5C). The production of both of these weak acids, including higher concentrations of acetate than lactate, indicates there are at least two subpopulations utilizing different metabolic pathways despite access to the same nutrient resources. One subpopulation utilizes a fully functional respiratory chain, very active glycolytic pathway, and robust Pta-AckA activity to rapidly metabolize glucose, as in aerobic conditions (Figure 3A). Meanwhile, another subpopulation is fermenting to produce lactate, as in microaerobic conditions (Figure 3B). The formation of these niches by the first timepoint further supports the notion of heterogeneity initiating before nutrient gradients can be established, as mature structures have not formed and there is a constant flow of fresh nutrients over these cells.

3.2 Metabolic gene reporters reveal differences in nutrient utilization

Population level analysis of metabolite concentrations revealed multiple niches within the *S. aureus* biofilm, but it didn't inform us about where or how these niches formed. To better understand spatiotemporal development of metabolic niches, we devised a fluorescent gene reporter approach that allowed us to track when metabolic pathways were activated, with the idea that expression of a metabolic gene is indicative of a metabolic pathway being activated. For this approach to work, we needed to look at genes under heavy transcriptional regulation, since our fluorescent reporters won't be responsive to other forms of metabolic regulation, such as allosteric regulation of the metabolic enzyme. For this reason, we chose *pfkA* to serve as our glycolytic reporter,

because it's promoter contains a putative catabolite responsive element (*cre*) site (190) in front of the transcription start site, indicating CcpA is an activator of *pfkA* expression (181). For our TCA cycle reporter, we chose the gene encoding the first enzyme of the pathway, *citZ*, which is directly repressed by CcpA (216). Choosing a reporter for the Pta-AckA pathway was difficult, as there is evidence of transcriptional regulation by CcpA in *B. subtilis,* but none identified in *S. aureus* yet (195, 217, 218). Reporters for both *pta* and *ackA* were made, but only the *ackA* reporter fusion was used in this study, as it showed upregulated expression when the Pta-AckA pathway was active (see below).

3.2.1 *pfkA*, *ackA*, *citZ*, and *ldh1* reporters were expressed when their respective pathways were activated

As mentioned above, In the presence of excess glucose and oxygen, *S. aureus* preferentially consumes glucose and produces acetate in the presence of excess glucose and oxygen. Once glucose is exhausted, *S. aureus* imports the acetate and converts it to acetyl-CoA, which is then used to fuel the TCA cycle and further growth (219). Since glycolysis and the Pta-AckA pathways are utilized during the exponential phase as described above, we expected a sharp increase in signal from our *pfkA* and *ackA* reporters during this time. As shown in Figure 4A, we observed exactly that: our glycolytic and Pta-AckA pathway reporters were working as expected and strongly fluoresced during the time frame when glucose is rapidly consumed from the media.

Furthermore, after glucose was depleted, acetate was consumed and used to fuel the TCA cycle, which had been derepressed as shown by our *citZ* reporter. These data validated our approach that transcriptional reporter fusions could be used as a tool for spatiotemporal analysis of metabolic pathway activation.

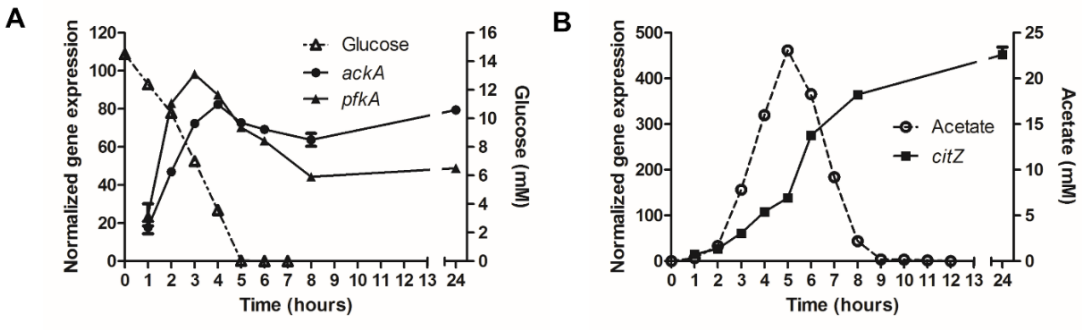

Figure 4. Validation of gene reporter approach using glycolysis, Pta-AckA pathway, and TCA cycle as model metabolic pathways. (A) Normalized gene expression from our gene reporter fusions (*pfkA*, *ackA*) was compared with media glucose levels to assess whether our approach reflected the metabolic status of cells. (B) Following glucose depletion, we assessed whether our *citZ* reporter reflected the increased TCA cycle activity during the post-exponential phase of growth when acetate is consumed to support further growth.

3.2.2 Expression of *pfkA* is stronger in large microcolonies

Previous studies have shown glycolytic genes are upregulated in biofilms, more so than their planktonic counterparts (220, 221). To examine glycolytic gene expression and ask whether there is differential expression of *pfkA* during biofilm development, we constructed a dual reporter fusion where the *cidABC* promoter drove expression of *dsRed* and the *pfkA* promoter controlled expression of *sgfp*. We chose to make a dual reporter so that we could tag the different niches that form during *S. aureus* biofilm development, where large towers express *cidABC* late in development when a substantial biomass has accumulated and small towers constitutively express *cidABC* (74).

As shown in Figure 5, we were fortunate enough to have both tower types develop in the same field of view, which allowed for a good comparison of glycolytic gene expression within these niches. Throughout the development of these biofilms, we observed a low level of constitutive *pfkA* expression. In the small tower, which is constitutively expressing *cidABC* (red), we observed no relative increase in *pfkA* expression (green), indicating this niche is not upregulating glycolysis to support its growth. However, in the large tower, which did not express *cidABC* until late in its development, we observed strong upregulation of *pfkA*, indicating the large tower niche requires increased expression of glycolytic genes to support its growth.

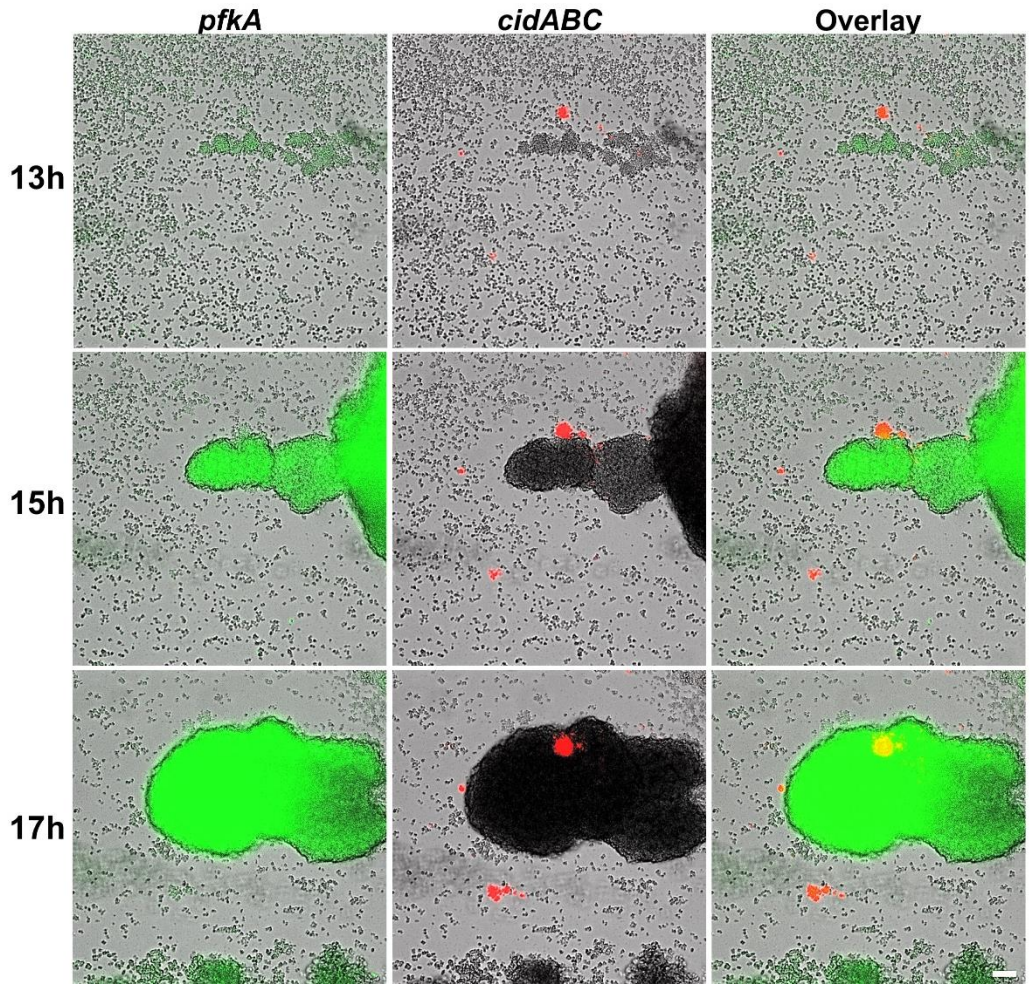

Figure 5. *pfkA* is constitutively expressed but strongest in large towers as they develop. A dual *pfkA::sgfp, cidABC::sDsRed* reporter was used to detect spatiotemporal changes in glycolytic activity during biofilm development. Large towers do not express *cidABC* until later in development, whereas small towers constitutively express *cidABC*. In the same field of view, we observed both a large and small tower develop, allowing a good comparison between these niches for glycolytic gene expression. Representative images are shown of large and small towers developing next to each other at 13h, 15h, and 17h.

3.2.3 Expression of *citZ* is limited to center of large microcolonies

In our microfluidic flow cell system, nutrients are constantly replenished. As a result, we did not expect to see much expression of our *citZ* reporter, since TCA cycle activity should be repressed (191). However, biofilms do not always follow cues from their environment due to their fundamental heterogeneous nature (66). Normally induced in hypoxic conditions, *cidABC* was nevertheless constitutively expressed in small towers despite an oxygen-rich environment (74), underscoring the physiological heterogeneity and diverse microenvironmental niches within biofilms.

Therefore, despite an environment replete with glucose and oxygen, we assessed TCA cycle activity during biofilm development using our gene reporter approach. As before, we used a dual reporter containing the promoter for *cidABC* driving expression of *dsRed*. This time, however, we fused the promoter for *citZ* to *sgfp*. As shown in Figure 6, we did not observe much *citZ* expression throughout biofilm development until the late stages of large tower formation, when the center of the biomass presumably becomes hypoxic. We have thought the center of these large towers are hypoxic due to the biomass presumably limiting oxygen diffusion to this area. Upregulation of *cidABC* expression supported this hypothesis (74). Transcriptional regulation of the TCA cycle is governed mostly by the presence of oxygen and the carbon source (213, 214), where the presence of glucose and/or the absence of oxygen cause transcriptional repression of the TCA cycle. Therefore, it is not clear why the TCA cycle is derepressed in the presumably hypoxic environment in the center of a large tower.

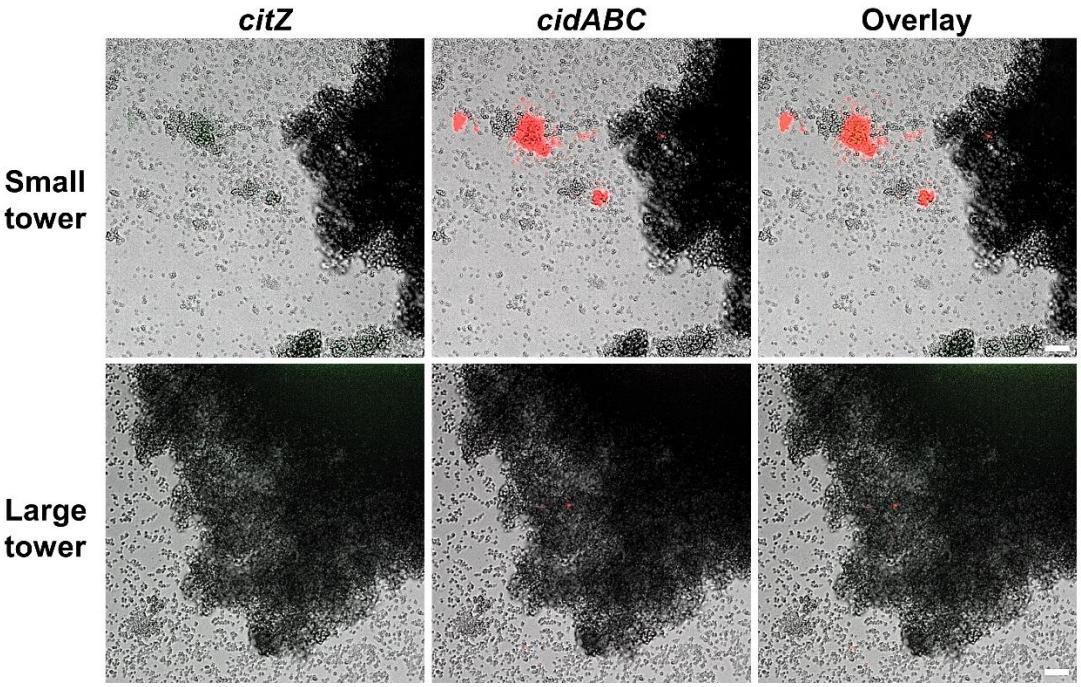

Figure 6. *citZ* is expressed in the center of large towers. A dual *citZ::sgfp, cidABC::sDsRed* reporter was used to detect spatiotemporal changes in TCA cycle activity during biofilm development. Small and large towers were observed in different fields of view, so representative images of small and large towers after 17h of growth are shown, with small towers in the top panels and large towers in the bottom panels.

3.2.4 The Pta-AckA pathway is important for large microcolony development

Finally, we looked at the expression of *ackA* during biofilm development. The Pta-AckA pathway is heavily utilized during *S. aureus* growth in excess oxygen and glucose (206), so at least a basal level of constitutive *ackA* expression was expected. In this experiment, we tagged tower types using Propidium Iodide (PI), which stains eDNA and dead cells, because only large towers incorporate eDNA and dead cells into their matrix (74). We observed a basal level of *ackA* expression, as expected, but also a strong upregulation of *ackA* expression in the large towers (Figure 7), similar to our observation of *pfkA* expression during large tower development (Figure 5). However, even stronger upregulation of *ackA* expression appeared in the center of the large towers. It's likely this niche within the center of mature large towers is microaerobic, as evidenced by *ackA* expression and *ldh1* expression (unpublished data), providing an example of how the microenvironment influences metabolic gene expression within biofilms (66).

These data also suggest the Pta-AckA pathway is critical for large tower development, since the pathway is upregulated during large tower development and the upregulation gets stronger after enough biomass has accumulated and the center becomes more hypoxic (Figure 7). In some unpublished work from our lab, inactivation of either *pta* or *ackA* leads to formation of biofilms lacking the *lrg*-expressing large towers (unpublished data), supporting the idea that the Pta-AckA pathway is critical for the development of large towers.

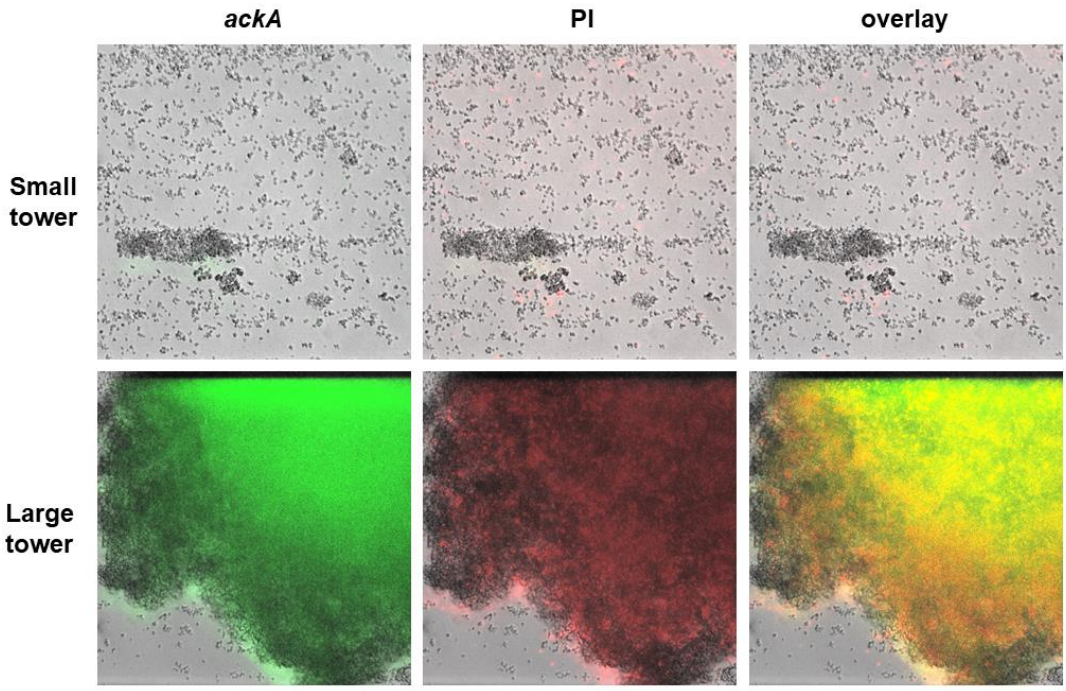

Figure 7. *ackA* is strongly expressed in large towers, especially within the center of the biomass. An *ackA::sgfp* reporter was used to investigate Pta-AckA pathway activity during biofilm development. Tower types were tagged with Propidium Iodide (PI), which stains eDNA and dead cells. Low constitutive *ackA* expression in the basal layer gave way to strong upregulated *ackA* expression in large towers but not small towers. Representative images after 17h of biofilm growth are shown.

3.3 Discussion

In this study, we sought to answer the question of how, where, and why physiological heterogeneity arises during biofilm development. Though we still do not understand the answers to this question, our findings revealed key characteristics about physiological heterogeneity within biofilms.

As Figure 3C shows, there are multiple metabolic niches that arise during biofilm development. Furthermore, the metabolic heterogeneity among these niches initiates from the first stages of biofilm development. Notably, this means the cells are within the same environmental conditions, suggesting heterogeneity is an innate strategy to physiologically diversify the population.

However, we also observed evidence that physiological heterogeneity arises due to the influence of the microenvironment. We observed increased *ackA* and *ldh1* expression within the center of mature large towers (Figure 7, unpublished data), indicating this niche is microaerobic (Figure 3A, 3B).

Regardless of the origin of physiological heterogeneity, it undoubtedly provides an advantage to the biofilm community. Biofilm bacteria are readily adaptable to extreme conditions, such as ultraviolet (UV) radiation, high or low temperature, high or low pH, high salinity, high pressure, and nutrient deprivation (222-226). One explanation for how biofilms can survive such harsh conditions is physiological heterogeneity, where there is always a subpopulation already adapted or ready to adapt to survive in a new environmental condition. For example, *B. subtilis* maintains approximately 10% of its population in a competent state, for the purpose of adapting to a new stress if one arises (91, 92). Furthermore, due to the population being in multiple metabolic states (e.g. growing, dormant, stress-adapted), biofilm bacteria can withstand pressures such as

antibiotic treatment (39, 227). This idea has been termed the “insurance hypothesis”, where diversity protects the community from unstable environmental conditions (228).

While physiological heterogeneity has been characterized in biofilms before, our study provides some insight into spatial and temporal changes that occur during biofilm development. We discovered physiological heterogeneity is both an innate process, where bacteria are hard-wired to differentiate into multiple metabolic states, as well as a response to microenvironmental cues, such as low oxygen conditions within large biofilm structures.

4 Interplay between CodY and CcpA in regulating central metabolism and biofilm formation in *S. aureus*.

Staphylococcus aureus is a leading cause of bacteremia, endocarditis, skin and soft tissue infections, and osteomyelitis (229). Along with the plethora of sites it can infect in the human body (180), *S. aureus* is resistant to several antibiotics and was listed in the High Priority category of the WHO’s global priority pathogen list (230). The adaptability of *S. aureus* to diverse environments can be attributed to the metabolic versatility of the organism and its ability to overhaul the regulatory networks governing metabolism and virulence (181, 182). It has been shown that *S. aureus* controls the expression of toxins, biofilm genes, and metabolic genes through the use of two global transcriptional regulators, CodY and CcpA, that sense and respond to environmental conditions (186, 192, 195-197, 199).

CodY is a global transcriptional regulator in Gram positive bacteria, directly or indirectly regulating over 200 genes, including numerous metabolic genes (183). CodY

activity is regulated by levels of branched chain amino acids (BCAAs) and GTP, tying its activity to nutrient availability. As nutrients become limited and levels of BCAAs and GTP decrease, CodY loses affinity for its targets, which are under repression by CodY (231). Promoters have varying affinities for CodY, typically grouped by their functions. DNA sequences with a higher affinity for CodY will continue to be repressed in conditions with slight nutrient limitation, and as conditions become more deplete of nutrients there is a stepwise derepression of CodY target genes (183). For example, nutrient transporters are derepressed first, followed by metabolic synthesis pathways, then virulence factors used to damage tissues and scavenge resources are derepressed (186). This stepwise regulation allows *S. aureus* to adapt to a wide variety of environments.

Carbon catabolite protein A (CcpA) is another global transcriptional regulator in Gram positive bacteria that is responsible for carbon catabolite repression (CCR) and carbon catabolite activation (190, 191). CcpA regulation can be glucose-dependent or -independent, where the majority of the genes undergo glucose-dependent regulation by CcpA (192). CcpA can form complexes with several partners, including HPr and CodY (193). When glucose enters the cells through the sugar phosphotransferase system (PTS), HPr is phosphorylated at a serine residue (Ser46), after which it can form a complex with CcpA. The CcpA-HPr-Ser46-P complex has increased affinity for catabolite responsive element (*cre*) sites (190), which is further enhanced by elevated levels of glucose-6-phosphate and fructose-1,6-bisphosphate (194). CcpA represses genes within the TCA cycle and secondary carbon source catabolism, such as amino acids, while activating genes encoding components of the glycolytic and fermentative pathways (195).

Like CodY, CcpA activity is regulated by environmental conditions, specifically through levels of fructose-1,6-bisphosphate (FBP) and glucose-6-phosphate (191).

Interestingly, the metabolic gene targets of CodY and CcpA meet at key nodes of central metabolism, such as amino acid biosynthetic pathways, the TCA cycle, and glycolysis (190, 192, 198). Together, these two regulators sense the nutritional environment and govern flow of carbon and nitrogen by controlling catabolic and anabolic pathways involved in sugar and amino acid utilization. Previous studies have implicated the importance of these metabolic regulators during biofilm formation. It has been shown that inactivation of *ccpA* results in a loss of biofilm biomass, though the *ccpA* mutants retain the ability to adhere to a surface (196, 197). Inactivation of *codY* has been found to either increase or decrease biofilm biomass, depending on the strain of *S. aureus* used in the study (187, 188). Atwood *et al.* attributed this to the strain-specific ability to produce poly-N-acetylglucosamine (PIA) polysaccharide, which is correlated with methicillin resistance (189). Inactivation of *codY* appears to decrease biofilm biomass in methicillin-resistant strains, which typically produce low amounts of PIA, whereas methicillin-sensitive strains typically produce PIA and form biofilms with very “stringy” structures tethered together by eDNA and PIA (68, 189). The operon encoding the biosynthetic machinery for producing PIA, *icaADBC*, is under direct repression by CodY. As a result, the *codY* mutant overproduces this positively charged matrix polysaccharide, which in turn acts as a sponge for negatively charged eDNA (68).

In the current study, we investigated the impact of CodY and CcpA inactivation on central metabolism and biofilm formation in *S. aureus*. Consistent with previous findings, we observed disrupted flow through central metabolic pathways, such as glycolysis and amino acid biosynthesis (185, 192, 195). Furthermore, rather than completely abrogate PIA production, disruption of carbon flow through inactivation of *ccpA* in a *codY* mutant only reduced PIA production. Despite a reduction in PIA production, the biofilm formed by a *codY ccpA* mutant contained the “stringy” structures, like the *codY* mutant, that are

held together by PIA and eDNA. However, upon treatment with DNase I, only the "stringy" structures within the *codY* mutant biofilms were disrupted whereas the "stringy" structures of the *codY ccpA* mutant biofilms remained intact, suggesting much less eDNA is incorporated into the matrix. Overall, disruption of central metabolism has a major impact on cellular physiology and proper biofilm development.

4.1 Growth characteristics of *codY*, *ccpA*, and *codY ccpA*

As master regulators in many Gram positive bacteria, CodY and CcpA play major roles during growth by modulating flow through key metabolic pathways, controlling toxin production, and coordinating biofilm development (68, 186, 192, 196, 197). Both of these regulators have been shown to interact with other regulators, including each other, so we wanted to investigate the interplay between them throughout the growth cycle (193). We started by growing planktonic cultures of the wild-type (UAMS-1) strain and the *codY*, *ccpA*, and *codY ccpA* mutant strains and performing hourly measurements of OD_{600} and extracellular pH (Fig. 8A). As shown in Fig. 8A, the *codY* mutant has a slight growth defect during the exponential phase of growth and the *ccpA* and *codY ccpA* mutants have a more pronounced growth defect that lasts until stationary phase. Furthermore, the *ccpA* and *codY ccpA* mutants fail to acidify the media during the exponential phase, in contrast to the WT and the *codY* mutant (Fig. 8A), indicating the *ccpA* and *codY ccpA* mutants do not produce as many weak acids during the exponential phase as the WT or the *codY* mutant. Using growth data between zero and three hours of growth, we calculated the doubling time for each strain (Fig. 8B). Previous studies have found the doubling time of *S. aureus* to be between 24-60 minutes, depending on the nutrient conditions (232). In our study, we found the WT had a doubling time of approximately 30 minutes in TSB supplemented with 0.25% glucose (Fig. 8B). Also, in accordance with the growth curve, we observed a slightly longer doubling time for the *codY* mutant, and

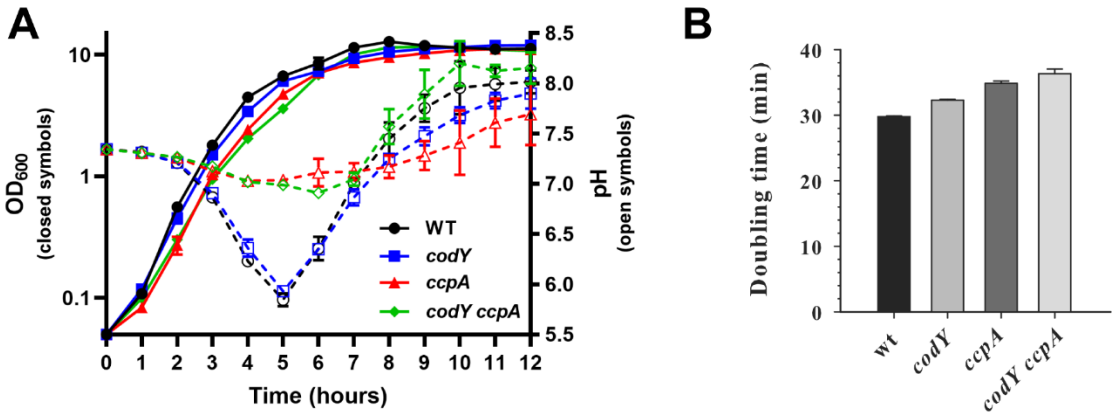

Figure 8. Growth characteristics of wild-type (WT) and the *codY*, *ccpA*, and *codY ccpA* mutants in TSB supplemented with glucose. (A) Each strain was cultured in TSB supplemented with 0.25% glucose and incubated for 12 hours at 37°C with shaking (250 rpm). Optical density (OD_{600}) and extracellular pH were measured hourly. (B) Using the change in OD_{600} between zero and three hours of growth (exponential phase), we calculated the number of new generations of bacteria and the doubling time for each strain.

even longer doubling times for the *ccpA* and *codY ccpA* mutants (Fig. 8B). In conclusion, inactivation of *codY* slightly impacts growth in TSB supplemented with 0.25% glucose, whereas inactivation of *ccpA* or both *codY* and *ccpA* resulted in a more significant growth impairment.

Next, we collected culture supernatants over the course of 12 hours of growth to analyze extracellular metabolites. First, we measured glucose concentrations and observed the *ccpA* and *codY ccpA* mutants were much slower to consume glucose, as expected since CcpA mediates carbon catabolite repression (Fig. 9A, (191)). Similarly, the *ccpA* and *codY ccpA* produced less acetate than the WT during the exponential phase, which explains the lack of media acidification observed in Fig. 8A (Fig. 9B). Though the change was much more subtle, the *codY* mutant showed a slight reduction in acetate production as well (Fig. 9B). Next, we measured ammonia production, since ammonia is produced from deamination reactions during amino acid catabolism (233). As expected, the *ccpA* and *codY ccpA* mutants produced more ammonia than the WT and the *codY* mutant during the exponential phase of growth, suggesting *ccpA* inactivation resulted in increased amino acid consumption due to disruption of carbon catabolite repression (Fig. 9C). Finally, since acetoin is a neutral molecule produced during overflow metabolism to prevent intracellular and extracellular acidification, we measured acetoin production (Fig. 9D). We observed a decrease in acetoin production in the *ccpA* mutant, suggesting CcpA is an activator of the *alsSD* operon encoding the enzymes required for acetoin production (234) Additionally, we observed a strong increase of acetoin production in the *codY* mutant, indicating CodY is a repressor of the *alsSD* operon.

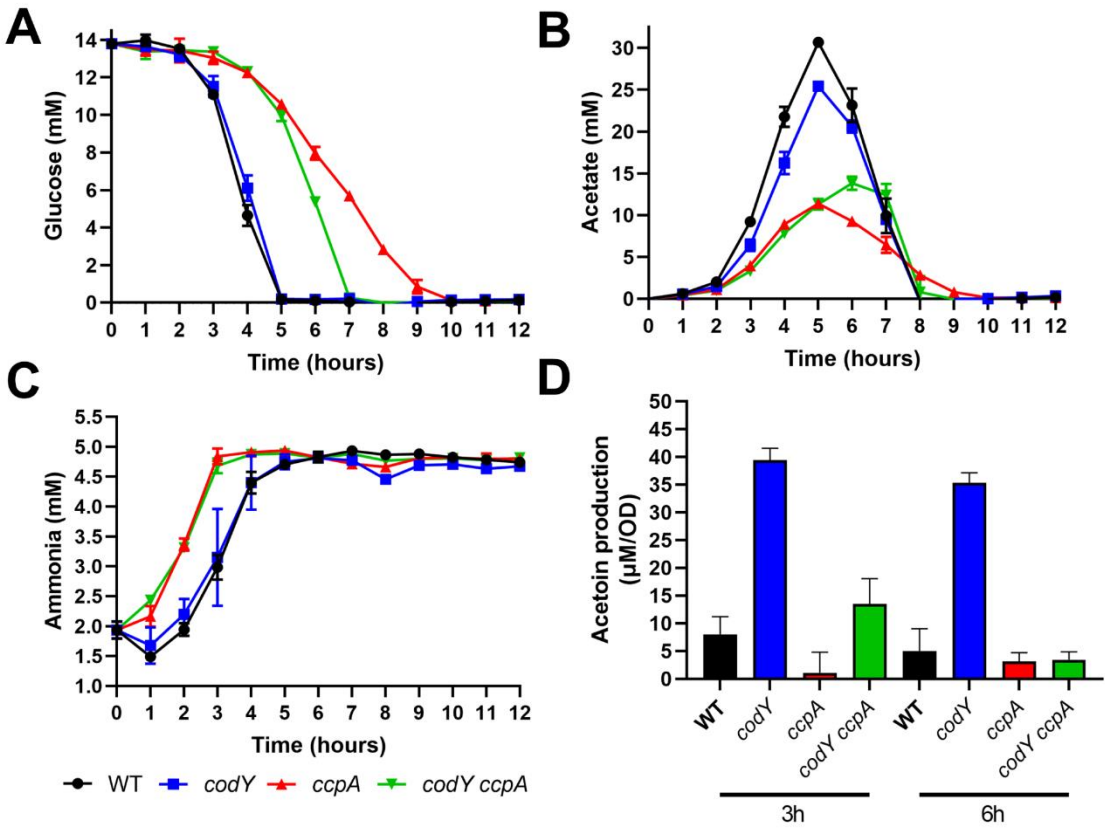

Figure 9. Analysis of extracellular metabolites reveals major changes to central metabolism as a result of *ccpA* and/or *codY* inactivation. (A) The *ccpA* and *codY ccpA* mutants consume glucose slower than the *codY* mutant and WT. (B) The *codY* mutant has a slightly lower yield of acetate produced during the exponential phase of growth, whereas the *ccpA* and *codY ccpA* mutant produce much less acetate than the WT. (C) The *ccpA* and *codY ccpA* mutants produce more ammonia during the exponential phase of growth, likely due to consumption of more amino acids compared to the WT. (D) The *codY* overproduces acetoin whereas the *ccpA* mutant appears to have decreased acetoin production.

4.2 Transcriptomic analysis reveals major changes to central carbon and nitrogen metabolism in *codY* and *ccpA* mutants

To gain a better understanding of the interplay between two master transcriptional regulators, we performed an RNA-seq analysis on the *codY*, *ccpA*, and *codY ccpA* mutants and compared them to the WT after three and six hours of growth. As mentioned earlier, CodY and CcpA regulate many central metabolic genes (185, 195). In Figure 10A, we show changes to metabolic gene expression after three hours of growth, when the cultures are in exponential phase and both regulators are active. Color-coordinated arrows indicate changes in metabolic gene expression for each mutant compared to the WT (Fig. 10A). Like Majerczyk *et al.*, we observed overexpression of genes involved in amino acid biosynthesis (*ilv-leu* operon), peptide and amino acid transport (*yveA*, *gmpC*, *gsiD*, *abgT*), toxin production (*hlgB*, *hlgD*, *lukF*, *lukH*, *seu*), and biofilm formation (*icaADBC*, *nuc1*, *sdrC*) in the *codY* mutant (Fig. 10A) (data not shown) (185). The *codY* mutant also showed a downregulation of *sucCD* expression, in contrast to the increase in *sucAB* expression that Majerczyk *et al.* observed in the *codY* mutant (185). It's not clear what caused this discrepancy, though further experiments in the next section would indicate *codY* has decreased expression of TCA cycle genes (Fig. 11A), suggesting CodY is a direct or indirect activator of the TCA cycle. Furthermore, we observed a decrease in purine metabolism (*pur* operon and *guaC*) and an increase in purine salvage expression (*xpt*) in the *codY* mutant (235) (Fig. 10A). Overall, our transcriptomic analysis supports the idea that CodY represses biosynthetic pathways in favor of utilization of nutrients from the environment (186).

As for the *ccpA* mutant, we observed decreased expression of glycolytic genes (*fda*, *fba*, *gpmA*) and virulence genes (*agrAD*, *seO*), consistent with results from previous studies on the CcpA regulon (192, 195, 199). Interestingly, our transcriptomic analysis

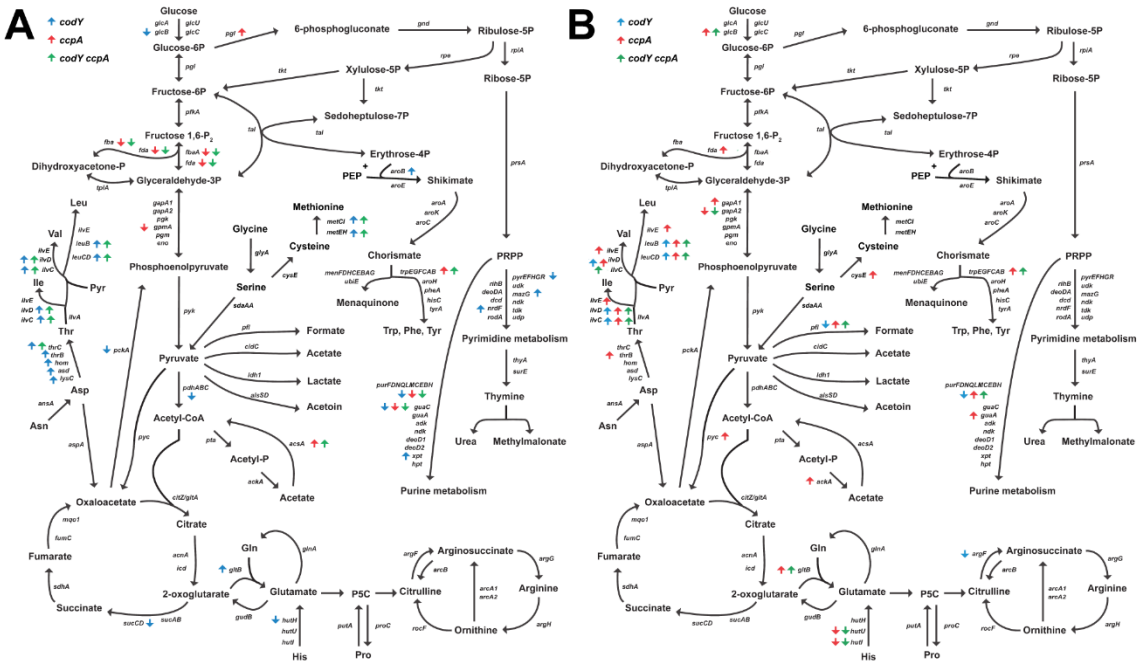

Figure 10. RNA seq analysis on metabolic genes reveals an interplay between CodY and CcpA to regulate metabolism. (A) Changes in metabolic gene expression compared to WT after three hours of growth are shown, with color-coordinated arrows indicating changes in the *codY* (blue), *ccpA* (red), and *codY ccpA* (green) mutants. (B) Changes in metabolic gene expression after six hours of growth are shown, with color-coordinated arrows depicting the changes in expression for each mutant compared to WT.

revealed increased expression of *pgl*, encoding the first enzyme of the Pentose Phosphate Pathway (PPP). A previous study showed the *gntRKP* operon was the only component of the PPP to be at least partially regulated by CcpA (195). The PPP is important for maintaining redox balance within the cell and produces components for nucleotide biosynthesis, suggesting CcpA plays a direct or indirect role in maintaining redox balance through the PPP (236). Additionally, we observed an increase in *acsA* expression, which catalyzes the reaction to make acetyl-CoA from acetate (Fig. 10A). A previous study by Seidl *et al.* did not detect significant changes to *acsA* gene expression in their transcriptomic analysis, but did observe increased levels of acetyl-CoA synthetase enzyme in the *ccpA* mutant (195). De-repression of *acsA* during exponential phase indicates *ccpA* is consuming secondary carbon sources such as acetate, even in the presence of excess glucose and oxygen. Further evidence of disruption to carbon catabolite repression is upregulation of peptide and amino acid transporters in the *ccpA* mutant, supporting our conclusion that deamination reactions during amino acid consumption are resulting in increased ammonia production by the *ccpA* mutant during exponential phase (data not shown, Fig. 9C).

In independent experiments, Majerczyk *et al.* and Seidl *et al.* observed CodY and CcpA involvement in regulation of purine metabolism (185, 195). We observed decreased purine biosynthesis in all of the mutants, suggesting purine biosynthesis is a tightly regulated pathway that is sensitive to changes in central metabolism (Fig. 10A). Since ATP is used as a substrate for the initial reactions of both pyrimidine and purine biosynthesis, the decrease in expression of these biosynthetic genes could be due to a lack of ATP in the mutant strain (237). At the three-hour time point, we indeed observed a small decrease in intracellular ATP levels for the *codY* mutant (Fig. 11). Since a purine salvage gene (*xpt*) is also upregulated, this would suggest the *codY* mutant is salvaging

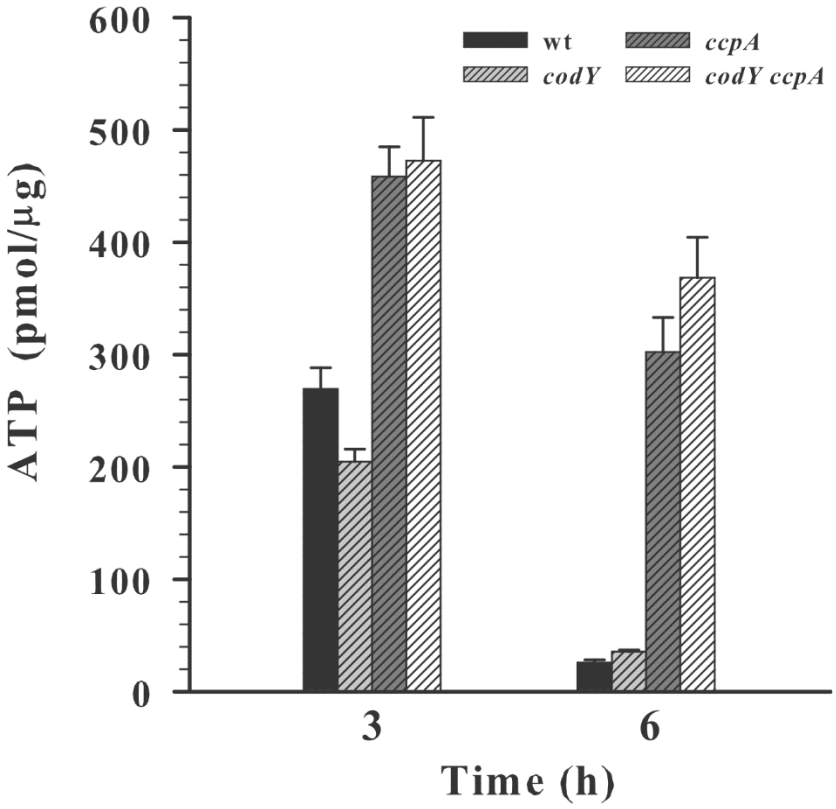

Figure 11. Measurement of intracellular pools of ATP reveals overabundance of ATP in the *ccpA* and *cod codY* mutants. Intracellular ATP concentrations were determined for the WT, *codY* mutant, *ccpA* mutant, and *codY ccpA* mutant after three and six hours of aerobic growth in TSB containing 0.25% glucose.

purines from the environment and displays decrease purine biosynthesis (Fig. 10A, Fig. 11). In the *ccpA* and *codY ccpA* mutants, however, there is an increase in ATP levels, in direct contrast to the hypothesis that ATP is limiting purine biosynthesis in these two strains (Fig. 11). Rather, since doubling time is increased in the *ccpA and codY ccpA* mutants (Fig. 8B), we believe these strains are downregulating purine biosynthesis to adjust to a slower growth. Furthermore, the TCA cycle is de-repressed and an abundance of NADH is available within the *ccpA* and *codY ccpA* mutants (218), leading to increased ATP levels despite slower growth, hence the need to downregulate purine biosynthesis.

The *codY ccpA* mutant shared characteristics with both single mutants and phenocopied each mutant in different ways. For example, the *codY ccpA* mutant exhibited decreased expression of glycolytic genes (like the *ccpA* mutant) and increased amino acid biosynthesis genes (like the *codY* mutant). As mentioned above, inactivation of *ccpA* resulted in decreased expression of the *agr* system, a master regulatory system for virulence gene expression in *S. aureus* (199, 238). Conversely, CodY represses the expression of *agr* and as a result there is overexpression of various *S. aureus* toxins in the *codY* mutant, including *hlgB*, *hlgD*, *lukF*, *lukH*, and *seu* (183, 185). Therefore, the *codY* and *ccpA* mutations have opposing effects on the expression of the key virulence factor regulatory gene, *agr*, resulting in opposing phenotypes for expression of toxin genes (199, 239). In our analysis, the double *codY ccpA* mutant did not show increased expression of toxins, indicating the *ccpA* phenotype of decreased toxin expression was dominant over the *codY* phenotype of overexpression of these toxins (data not shown). These data indicate direct or indirect activation of the *agr* locus by CcpA is required for toxin expression, regardless of CodY repression of *agr*. Similarly, the derepression of biofilm formation genes (*ica, nuc,* or *sdrC*) caused by inactivation of *codY* was ablated in

the *codY ccpA* mutant, again indicating the effect of *ccpA* mutation was dominant over the effect of *codY* mutation (data not shown).

Altogether, during the exponential phase of growth when nutrients are abundant, CodY and CcpA reduce carbon flow from secondary carbon sources and shut down toxin production to optimize growth (Fig. 10A, data not shown). Inactivation of these metabolic regulators has detrimental effects to exponential phase growth (Fig. 8A,B, Fig. 9A-D).

During the post-exponential phase of growth, when the WT has depleted glucose and is utilizing acetate to fuel the TCA cycle to support further growth, we observed some interesting differences in the *codY*, *ccpA*, and *codY ccpA* mutants. Due to slower growth and glucose consumption (Fig. 8A,B, Fig. 9A), the *ccpA* and *codY ccpA* mutants still have glucose available to them at this time-point (six hours). As a result, we observed several differences between the WT, the *ccpA* mutant, and the *codY ccpA* mutant. First, we observed increased expression of the PTS glucose transporter *glcB* in both the *ccpA* and *codY ccpA* mutants (Fig. 10B). However, we only observed increased expression of glycolytic genes (*fda*, *gapA1*) in the *ccpA* mutant, indicating CodY may be required for activation of glycolytic gene expression during the post-exponential phase. Additionally, we observed decreased expression of the gluconeogenic gene *gapA2* in the *ccpA* and *codY ccpA* mutants, which is logical since glucose is still available to them whereas glucose is exhausted from the media for the WT (Fig. 9A, Fig. 10B). Furthermore, pathways for carbon overflow (*pfl*) were overexpressed in the *ccpA* and *codY ccpA* mutants, indicating increased flux from the central carbon metabolite pyruvate compared to the WT. Finally, the *ccpA* mutant showed increased *ackA* expression, which encodes the second enzyme of the Pta-AckA pathway, which is critical for production of acetate during growth in excess glucose and oxygen (206).

These observations can be attributed to differences in glucose availability between the WT and the *ccpA* and *codY ccpA* mutants.

The main differences between the WT and the *codY* mutant in the post-exponential phase was the increased expression of amino acid biosynthesis genes (*ilv-leu* operon) and proteases (*aur*, *sspB*, *sspC*) and the decreased expression of *pfl* (formate production) and the *pur* operon (purine biosynthesis) in the *codY* mutant (Fig. 10B, data not shown). These data indicate amino acids are still available to the WT and CodY plays a role repressing exoprotease expression (that would scavenge nutrients from the host) as well as amino acid biosynthesis during the post-exponential phase of growth (Fig. 10B, data not shown).

4.3 Targeted gene expression analysis reveals CodY and CcpA coordinate metabolism and virulence

To validate the RNA-seq findings and to get a closer look at gene expression at key metabolic nodes, we performed RT-PCR on select gene targets (*pgi*, *pfkA*, *pdhA*, *ackA*, *citZ*, *pyc*, *glmU*, *icaA*, *ldh1*, *alsS*, *cidA*, *ilvD,* and *RNAIII*) after three and six hours of growth (Fig. 12A-B). We observed consistent patterns with the RNA-seq data for exponential-phase cells, including decreased expression of glycolytic genes across all three mutants compared to the WT, with the exception of *pfkA* in the *codY* mutant (Fig. 12A). Furthermore, the *codY* and *codY ccpA* mutants demonstrated increased expression of *ilvD*, which validates the increased amino acid biosynthesis genes seen in the RNA-seq analysis. We also saw that the *codY* mutant had decreased expression of *citZ*, the gene encoding the first enzyme of the TCA cycle, similar to the decreased expression of the TCA cycle operon *sucCD* expression observed in the RNA-seq analysis. The *ccpA* mutant, on the other hand, showed increased expression of *citZ*,

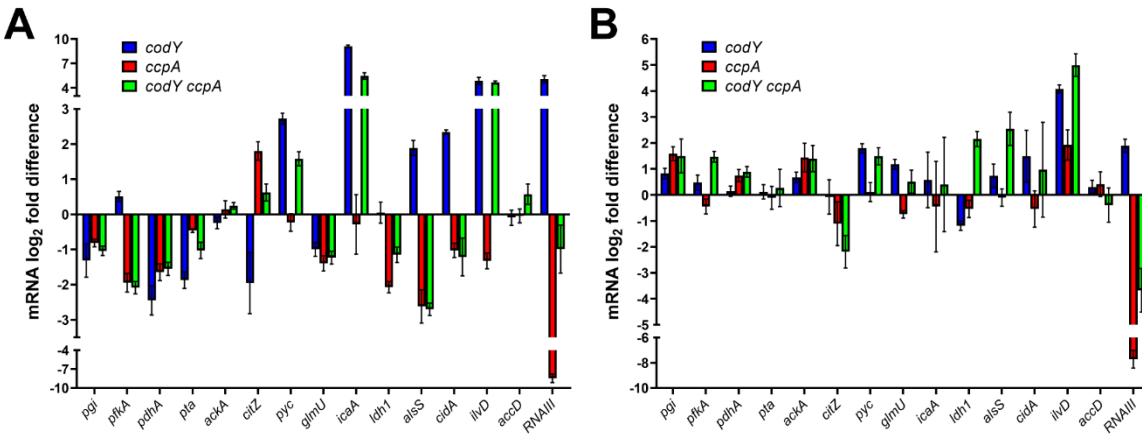

Figure 12. Expression of various genes corroborates RNA-seq results. RT-PCR was performed on the same mRNA samples collected for RNA-seq using primers to analyze expression of key metabolic genes and RNAIII. Differences in gene expression between each mutant and the WT after three hours of growth (A) or six hours of growth (B) are shown.

consistent with previous studies that have shown *citZ* to be repressed by CcpA (Fig. 12A) (195).

Using RT-PCR, we found changes in gene expression that were not identified in the RNA-seq analysis. For example, RT-PCR analysis of *icaA* expression after three hours of growth showed increased expression in the *codY* and *codY ccpA* mutants, in contrast to the RNA-seq analysis that only showed a significant difference of *icaA* expression in the *codY* mutant (Fig. 12A, data not shown). Additionally, although we did not detect any significant changes in *pyc* expression in the RNA-seq analysis (data not shown), we found an increased *pyc* expression in the *codY* and *codY ccpA* mutants, which was consistent with a previous transcriptomics analysis (Fig. 12A) (185). Furthermore, we detected lower gene expression of pyruvate fermentation pathway genes (*ldh1*, *alsS*, *cidA*) in the *ccpA* and *codY ccpA* mutants using RT-PCR, also consistent with results from a previous transcriptomic study (Fig. 12A) (185). There was also decreased *pta* expression in the *codY* and *codY ccpA* mutants, but no changes in *ackA* expression in any of the mutants. Seidl *et al.* did not observe any changes to *pta* or *ackA* expression in a *ccpA* mutant (195), though Shivers *et al.* observed both CodY and CcpA are positive regulators of *ackA* in *B. subtilis* (198). We also observed decreased *glmU* expression in all strains, similar to the decrease in glycolytic gene expression (Fig. 12A). *glmU* is a key enzyme in the synthesis of UDP-N-acetylglucosamine (UDP-GlcNAc), an important precursor for cell wall synthesis and PIA production (210). In a subsequent section, we will show that the decreased *glmU* expression does not impair PIA production in the *codY* and *codY ccpA* mutants (Fig. 14A). Finally, in correlation with the RNA seq results, *RNAIII* was overexpressed in the *codY* mutant compared to the WT (Fig. 12A). In addition, *RNAIII* expression was strongly downregulated in the *ccpA* mutant. In accordance with our findings that virulence genes are not overexpressed in a double

codY ccpA mutant, we observed decreased *RNAIII* expression in the *codY ccpA* mutant, verifying CcpA is required for activation of the *agr* system even if repression by CodY is alleviated (Fig. 12A).

During the post-exponential phase of growth, the *ccpA* and *codY ccpA* mutants shoed increased glycolytic gene expression (*pgi*, *pfkA*, *pdhA*), except for *pfkA* expression in the *ccpA* mutant, which was slightly lower than WT (Fig. 12B). As mentioned before, glucose is still available for these strains, so an increase in glycolytic gene expression compared to the WT was expected (Fig. 9A). Similarly, we observed an increase in *ackA* expression for both the *ccpA* and *codY ccpA* mutants, in contrast to the RNA-seq data which suggested only the *ccpA* mutant had increased *ackA* expression (Fig. 10B, Fig. 12B). Since glucose is exhausted for the WT by this point, the TCA cycle is derepressed. Since part of CcpA's role in carbon catabolite repression is to repress the TCA cycle, one might expect TCA cycle gene expression to be similar between the WT and the *ccpA* mutant during post-exponential phase of growth (191). However, we observed decreased *citZ* expression in the *ccpA* and *codY ccpA* mutants compared to the WT. These data would suggest that derepression of the TCA cycle through *ccpA* inactivation is not as strong as derepression caused by exhaustion of glucose, indicating the presence of one or more additional factors repressing the TCA cycle when glucose is present.

As before, we see patterns emerge where the *codY* mutant phenotype is dominant in the *codY ccpA* mutant as well as the opposite where the *ccpA* mutant phenotype is dominant. Again, the *codY* mutant phenotype is dominant in amino acid biosynthesis (*ilvD*) (Fig. 12B). However, now the *ccpA* mutant phenotype is dominant in expression of glycolytic genes (*pgi*, *pdhA*), *ackA*, and *RNAIII* (Fig. 12B). Overall, the RT-PCR data supported the findings of the global transcriptomic approach, where CcpA modulates

carbon catabolite repression and virulence gene expression and CodY modulates amino acid biosynthesis and virulence.

4.4 A metabolomic approach further elucidates pathways disrupted by CodY and CcpA inactivation

Next, we evaluated disruption to global metabolism caused by inactivation of the *ccpA* and *codY* genes by measuring intracellular metabolite concentrations after three and six hours of growth using LC/MS-MS (Fig. 13A,B). Generally, the observed differences between the mutants and UAMS-1 correlated with differences observed in the transcriptomic analysis.

During the exponential phase of growth, the *codY* mutant had elevated concentrations of intracellular amino acids, PPP intermediates, and nucleic acid intermediates (Fig. 13A). Increased intracellular amino acid concentrations are consistent with the increased expression of amino acid biosynthesis genes (Fig. 10A, Fig. 13A). RNA seq revealed decreased expression of purine biosynthesis genes in the *codY* mutant, yet here we observed increased concentrations of PPP intermediates and nucleic acid intermediates (Fig. 10A, Fig. 13A). As mentioned before, lower ATP levels in the *codY* mutant could explain the impairment of purine biosynthesis. Allosteric feedback inhibition by increased AMP levels in the *codY* mutant could cause downregulation of purine biosynthesis genes (240). The increased levels of purine intermediates could be explained by overexpression of purine salvage genes, such as *xpt* (data not shown).

Meanwhile, the *ccpA* mutant had increased concentrations of intracellular glycolytic intermediates, ornithine, 6-phospho-D-gluconate, and hypoxanthine. Meanwhile, the

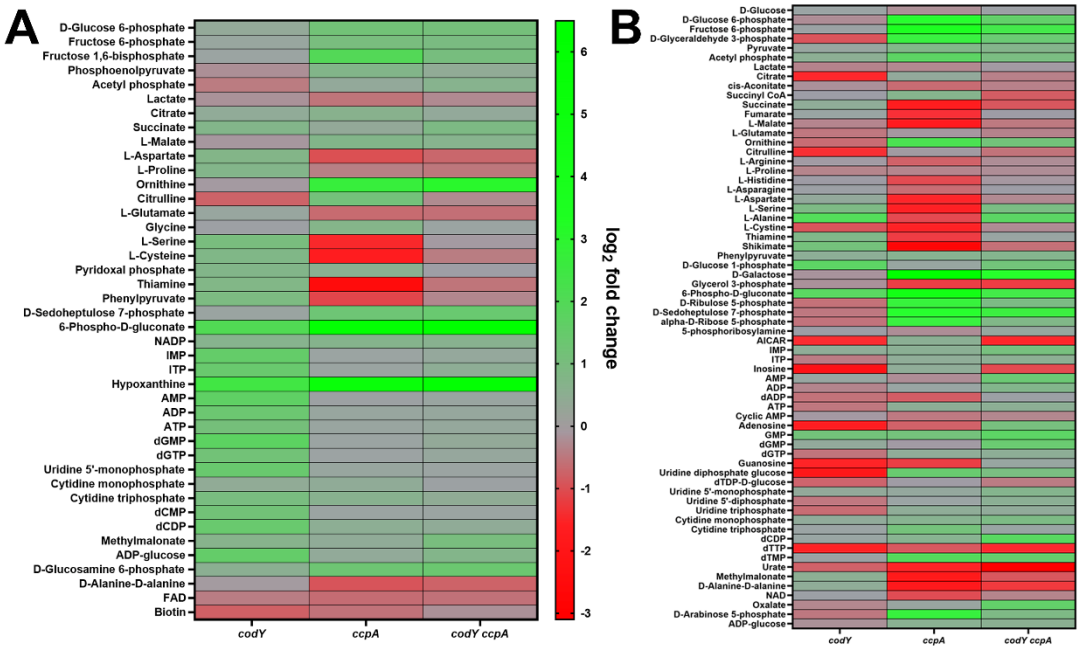

Figure 13. Metabolomics further elucidates metabolic changes resulting from *codY* and/or *ccpA* inactivation. (A) Fold-change differences greater than 2 at the three-hour time point are shown, with metabolites roughly grouped by pathway. (B) Fold-change differences greater than 2 at the six-hour time point are shown.

ccpA mutant had decreased intracellular levels of amino acids, consistent with our other data that suggest the *ccpA* mutant is consuming amino acids for growth during the exponential phase (Fig. 9C, Fig. 10A, Fig. 13A). For the most part, the trends of intracellular metabolite concentrations are similar between the *ccpA* and *codY ccpA* mutants (Fig. 13A). In the case of the *ccpA* and *codY ccpA* mutants, it appears as if there are specific blockages to certain pathways (PPP and purine biosynthesis), since these highly concentrated metabolites lay at nodes connecting central metabolic pathways and the other metabolites within those pathways show no change compared to WT, indicating a direct transcriptional regulatory role for CcpA (Fig. 13A).

Interestingly, like the *ccpA* mutant where the TCA cycle is derepressed, the *codY* mutant demonstrated a similar increase in citrate and succinate levels, despite decreased expression of TCA cycle genes in the *codY* mutant (Fig. 10A, Fig. 13A). It's not yet clear what role CodY has in regulation of the TCA cycle. One possible explanation could be that CodY is a direct or indirect activator of the TCA cycle. Without it, TCA cycle metabolites accumulate due to blockages caused by a failure to activate TCA cycle gene expression. In contrast, CcpA is a repressor of the TCA cycle and alleviation of this repression results in increased flux through the TCA cycle (218).

Finally, *ccpA* and *codY ccpA* showed decreased concentrations of D-alanine-D-alanine, indicating a defect in cell wall biosynthesis (Fig. 13A). There was a concomitant increase in D-glucosamine 6-phosphate concentrations in *ccpA* and *codY ccpA*, possibly due to a block in cell wall biosynthesis as indicated by decreased D-alanine-D-alanine. Inactivation of *ccpA* has been linked to cell wall alterations in previous studies (199, 241). The cell wall fraction of a *ccpA* mutant was compared with the wild-type *S. pneumoniae* strain and the authors found many cell wall proteins were regulated, directly or indirectly, by CcpA (241). Furthermore, another study showed that a deletion of *ccpA*

in the *S. aureus* strain COLn caused a four-fold reduction in susceptibility to oxacillin, an antibiotic that targets the cell wall (199). These findings, along with our own, suggest CcpA plays a role in cell wall biosynthesis.

Altogether, our results have indicated CodY and CcpA are master regulators of both metabolism and virulence gene expression during growth, all of which impacts the optimal growth of the organism.

4.5 Disruption of carbon flow through ccpA inactivation has only a minor effect on PIA production

Since inactivation of the *codY* gene is known to increase PIA biosynthesis through overexpression of the *ica* operon (183), we asked if disruption of central metabolism through *ccpA* inactivation resulted in decreased PIA biosynthesis. Earlier, in our RT-PCR analysis, we discovered *icaA* gene expression was comparable between the *codY* and *codY ccpA* mutants. However, carbon flow disruption could still impact the ability of the double *codY ccpA* mutant to produce PIA, so we directly measured PIA production using anti-PIA antibodies. As shown in Fig. 14A and 14B, there was only a slight reduction in PIA production in the *codY ccpA* mutant compared to the *codY* mutant. Notably, the

production of PIA in the *codY ccpA* mutant was still very high compared to the WT or *ccpA* mutant, indicating this overproduction of PIA by the *codY ccpA* mutant could result in a similar biofilm phenotype to the *codY* mutant.

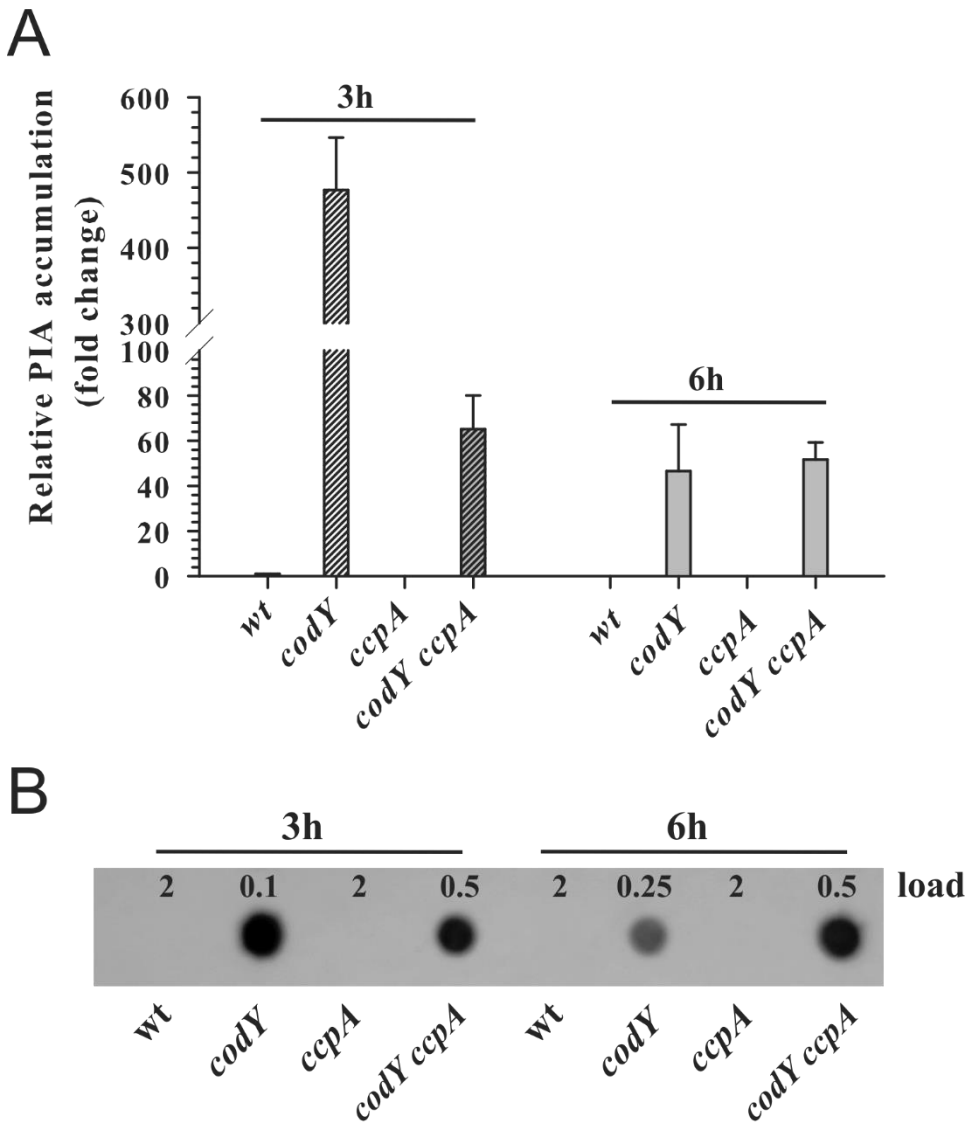

Figure 14. The *codY* and *codY ccpA* mutants overproduce PIA. Using anti-PIA antibodies, we detected PIA production by each strain after three or six hours of growth. Relative fold-change differences between each mutant and the WT are shown in (A) and the immunoblot used to quantify these differences is shown in (B).

4.6 Disruption of metabolic regulation alters biofilm matrix production and biofilm morphology

Finally, we tested the ability of these strains to form biofilms and the effect of *codY* and *ccpA* inactivation on biofilm matrix production. The *codY* mutation has been shown to cause the cells to form a biofilm with a matrix consisting of PIA and eDNA, with very “stringy” structures (68). Consistent with this, the biofilms formed by this mutant stained strongly with TOTO-1, a fluorescent probe that indicates the presence of eDNA and dead cells (242). After 6 hours of biofilm growth in a constant flow environment, we added matrix-degrading agents to test the biofilm matrix composition (Fig. 15). To disrupt proteins in the matrix, we added Proteinase K, which completely disrupted the UAMS-1 and *ccpA* mutant biofilms, whereas the *codY* and *codY ccpA* mutant biofilms remained relatively intact, with only the basal layer of cells being disrupted. The remaining biofilm cells were associated with the long “stringy” structures previously described (68). These remaining structures were presumably held intact by the increased levels of PIA as a result of *codY* inactivation. In contrast, DNase I treatment did not have a drastic effect on the basal layer of the biofilms formed by any strain but disrupted the “stringy” structures formed by the *codY* mutant, indicating the presence of eDNA in these structures. Interestingly, the *codY* mutant overexpresses *nuc*, which encodes a secreted nuclease that degrades matrix eDNA and is involved in the “exodus” phase of biofilm development (25). In agreement with the low eDNA staining, the *codY ccpA* mutant biofilm “strings” were not disrupted by DNase I treatment, presumably because they are held intact by PIA. Next, we used sodium metaperiodate to degrade matrix-associated PIA. As shown in Fig. 15, the “stringy” structures produced by the *codY* and *codY ccpA* mutant biofilms were disrupted by metaperiodate, indicating PIA is a major structural component for these structures.

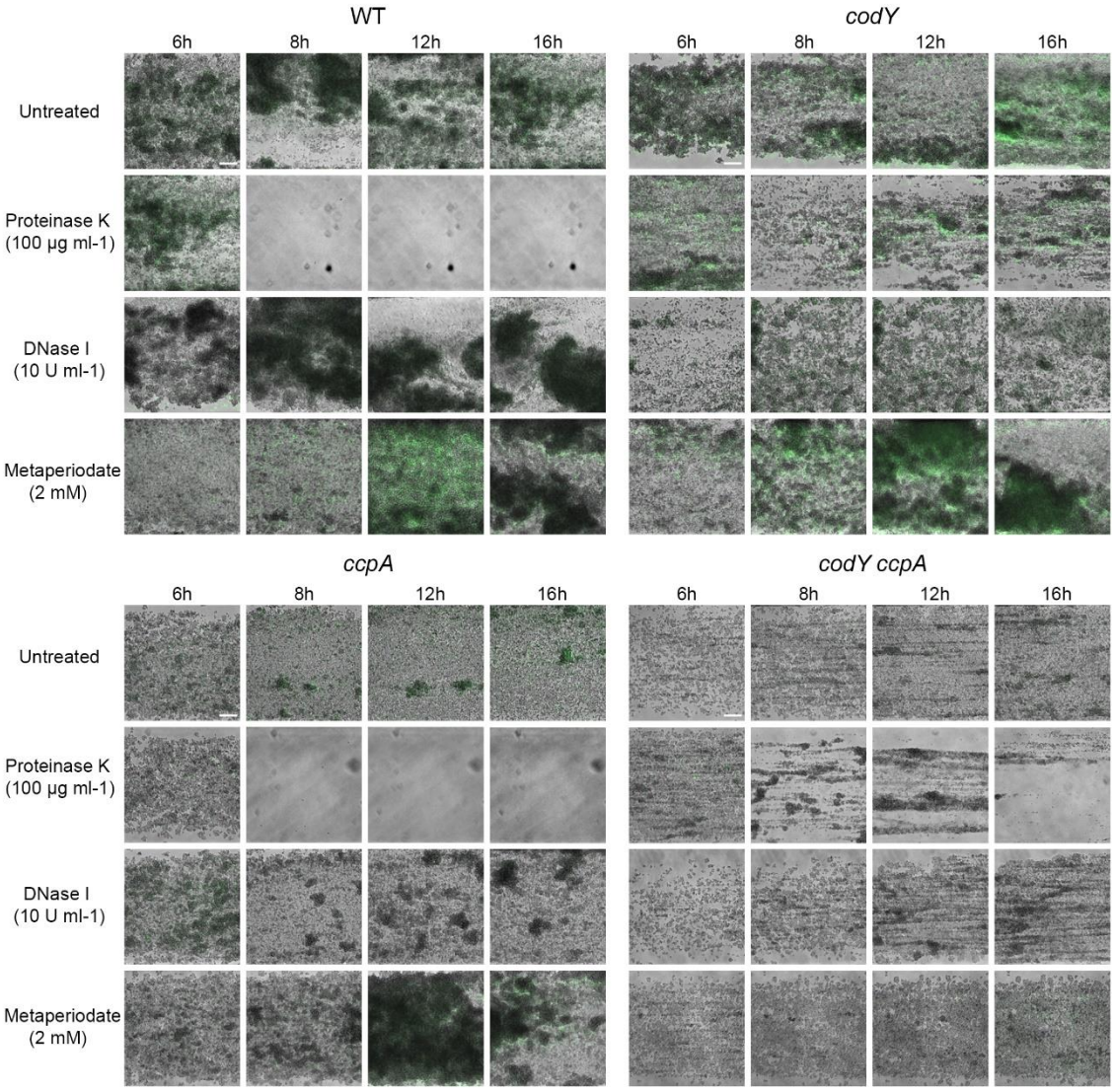

Figure 15. Metabolic regulation is critical for proper biofilm development. Each quadrant shows how each strain (WT, *codY*, *ccpA*, and *codY ccpA*) forms a biofilm in untreated conditions or when exposed to treatment with a matrix-degrading agent [Proteinase K (100 µg ml^{-1}), DNase I (10 U ml^{-1}), or sodium metaperiodate (2 mM)]. To further determine matrix production, we stained the biofilms with TOTO-1, which fluoresces green when it interacts with eDNA or dead cells.

Overall, the biofilm matrix produced by UAMS-1 likely consists of PIA, eDNA, and proteins, with proteins being the most crucial matrix component. In the *codY* mutant, the basal biofilm layer attaches through protein-substrate interactions and the “stringy” structures produced by the *codY* mutant are held together by PIA and eDNA. The *ccpA* mutant incorporates relatively little eDNA compared with all other strains, and with most of the matrix composition being proteins. The *codY ccpA* mutant exhibits an intermediate biofilm that incorporates relatively little eDNA in its matrix, the basal layer attaches via proteins, and the “stringy” structures are held together by PIA (but not eDNA, in contrast to the *codY* mutant). Clearly, metabolic regulation by CodY and CcpA are important for the development of a healthy, structured biofilm.

4.7 Discussion

Carbon catabolite repression (CCR) is well-conserved among bacteria, common to both Gram negative and Gram positive bacteria (243). In Gram positive bacteria, the transcriptional regulator CcpA, along with other components of CCR (HPr, HPrK, PTS), mediates the connection between environmental input (availability of glucose) and transcription of genes involved in consumption of glucose or secondary carbon sources (191). Additionally, another transcriptional regulator, CodY, modulates the production of toxins, amino acids, and biofilm matrix components like PIA (186). CodY is also sensitive to environmental input, as low concentrations of GTP or isoleucine causes CodY to lose its affinity for DNA in a step-wise fashion, allowing for de-repression of toxin, amino acid, and PIA biosynthesis (183). Together, these regulators must work to sense the environment and transduce those signals to modulate gene expression in the cell that allows for optimal growth and/or survival.

In this study, we found that inactivation of the *codY* and *ccpA* genes can drastically change expression of genes involved in central metabolism and virulence (Fig. 10A,B). Our findings confirm WT *S. aureus* preferentially consumes glucose to produce acetate (Fig. 9A,B) during the exponential phase of growth, producing ATP through substrate level phosphorylation and recycling NAD+ through the electron transport chain (ETC). When CcpA is inactivated, glucose consumption decreases while consumption of secondary carbon sources, such as amino acids and acetate, increases (Fig. 9A, Fig. 10A, Fig. 13A, data not shown). Inactivation of *codY* has small impact on growth during the exponential phase, with a slight reduction in acetate production (Fig. 9B) and increased amino acid biosynthesis (Fig. 10A). The double *codY ccpA* mutant grew similarly to the *ccpA* mutant, with increased consumption of secondary carbon sources and decreased glycolysis (Fig. 8A, Fig. 9A,B, Fig. 10A,B), but also exhibited increased amino acid biosynthesis like the *codY* mutant (Fig. 10A,B).

Another interesting finding was that CcpA is seemingly required for activation of the *agr* system (Fig. 12A,B, data not shown). Even though *codY* inactivation derepresses the *agr* system and causes overexpression of virulence factors, inactivation of *ccpA* was the dominant phenotype in the double *codY ccpA* mutant. In the *ccpA* mutant, we observed a strong decrease in expression of the *agr* system effector molecule, *RNAIII*, which stayed consistent in the *codY ccpA* mutant (Fig. 12A,B). This interplay for control of the expression of this major virulence regulator (*agr*) highlights the complexity and importance of gene regulation within *S. aureus* and how the regulators interact in ways to fine-tune expression of critical genes such as those encoding virulence factors.

Finally, we demonstrated that these regulators are important for the proper development of mature biofilm structures. Wild-type UAMS-1 forms highly structured biofilms containing various niches with unique morphologies, including differences in

gene expression and matrix composition, which are completely susceptible to Proteinase K treatment (Fig. 15, (25, 74)). In contrast, the *codY* mutant is known to make “stringy” biofilm structures held together by increased amounts of PIA and eDNA (68). In these experiments, we observed the *ccpA* mutant biofilms incorporate less eDNA into the matrix. In a double *codY ccpA* mutant biofilm, “stringy” biofilm structures are still formed but they incorporate less eDNA, as evidenced by the recalcitrance of these structures to DNase I treatment (Fig. 15). Proper regulation of metabolism and biofilm-related genes by CodY and CcpA is critical for biofilm development, as inactivation of either or both regulators drastically change the structure and composition of *S. aureus* biofilms. Though this study shed light on the interaction between CodY and CcpA in regulating central metabolism, virulence, and biofilm development, there is much to be learned about the complex interactions between these regulators and the roles they play during infection.

5 Discussion and Future Directions

Biofilm development is an intricately complicated process that is largely conserved among different bacterial species. Most species will attach to a surface, build an extracellular matrix and multiply, then partially degrade the matrix and disperse a subpopulation to colonize elsewhere. The molecular components used to mediate each stage differs among species, but some common features remain. Each species uses a combination of eDNA, polysaccharides, and/or proteins to form the biofilm matrix. The architecture provided by the matrix allows for the bacteria to form large structures, within which metabolically distinct microenvironments can form. From these microenvironments emerge heterogeneous gene expression, matrix production, and antibiotic susceptibility. However, observations in *P. aeruginosa* and *S. aureus* indicate physiological

heterogeneity is established well before any obvious microenvironment has a chance to form, indicating heterogeneity is a part of the developmental process and not just the byproduct of microenvironmental cues (24, 74, 112). Furthermore, the ubiquity of physiological heterogeneity among bacterial species implies that this behavior serves important functions. Thus, understanding the mechanisms behind physiological heterogeneity can help us develop better treatments for biofilm infections. Based on the data gathered to date, it seems clear that biofilm heterogeneity arises as a function of both microenvironmental and genetic factors. While the former can be predicted based on our knowledge of the response of bacteria to environmental signaling, the latter has eluded detection until relatively recently.

If some aspects of biofilm heterogeneity have a genetic basis, then what are the forces that underlie selection for these processes? One possibility is as a mechanism to conserve energy, whereby selected individuals make a shared product for the common good of the entire population. Examples of this are the division of labor for the production of the TasA protein and EPS matrix components in B. subtilis (19), or virulence factor expression by S. aureus (109). In both examples, key stages of biofilm development are (or are suspected to be) under the control of bistable switches that generate a heterogeneous response.

Another driving force selecting for heterogeneous expression are the benefits of a bet hedging strategy to prepare for an uncertain future. As mentioned above, persisters are frequently observed in biofilms (39). As is the case for adhesion and matrix production, antibiotic tolerance is under the control of bistable switches, likely as a means to prepare the population for unanticipated environmental threats. The presence of these persister cells allows the population to survive until either the community adapts their gene expression to the new conditions, or the adverse conditions improve. A

physiologically diverse biofilm can better withstand changing environmental stresses, such as nutrient limitation or the presence of antibiotics, similar to how a diverse forest can better withstand droughts and disease (244).

Future studies are sure to find more examples of bistable switches regulating the development and survival of biofilms. Physiological heterogeneity provides the biofilm population with the ability to survive stressful situations, giving rise to a formidable foe already adapted to our current methods of treatment. In the experiments described in this dissertation, we demonstrated that metabolic heterogeneity can arise stochastically before nutrient gradients can be established. Furthermore, we showed that metabolic regulation by CodY and CcpA are critical to the proper development of a mature biofilm, with control over the production of virulence factors and biofilm matrix components. In the future, we will investigate if physiological heterogeneity is disrupted by inactivation of metabolic regulators. We will utilize our gene reporter fusion approach to ask whether metabolic regulation plays a role in the establishment of metabolically distinct niches during *S. aureus* biofilm development.

Despite many advances in our understanding of biofilms, we are still just scratching the surface into the mechanisms underlying biofilm development and physiological heterogeneity. Armed with a better understanding of these mechanisms we will be better able to develop more informed therapeutic strategies to treat biofilm-associated infections.

Bibliography

1. Henrici AT. 1933. Studies of Freshwater Bacteria: I. A Direct Microscopic Technique. J Bacteriol 25:277-87.
2. Geesey GG, Richardson WT, Yeomans HG, Irvin RT, Costerton JW. 1977. Microscopic examination of natural sessile bacterial populations from an alpine stream. Can J Microbiol 23:1733-6.
3. O'Toole G, Kaplan HB, Kolter R. 2000. Biofilm formation as microbial development. Annu Rev Microbiol 54:49-79.
4. Costerton JW, Lewandowski Z, Caldwell DE, Korber DR, Lappin-Scott HM. 1995. Microbial biofilms. Annu Rev Microbiol 49:711-45.
5. Dodd MS, Papineau D, Grenne T, Slack JF, Rittner M, Pirajno F, O'Neil J, Little CT. 2017. Evidence for early life in Earth's oldest hydrothermal vent precipitates. Nature 543:60-64.
6. Klein F, Humphris SE, Guo W, Schubotz F, Schwarzenbach EM, Orsi WD. 2015. Fluid mixing and the deep biosphere of a fossil Lost City-type hydrothermal system at the Iberia Margin. Proc Natl Acad Sci U S A 112:12036-41.
7. Lutz RA, Kennish MJ. 1993. Ecology of deep-sea hydrothermal vent communities: A review. Reviews of Geophysics 31:211-242.
8. Ruby EG, Wirsen CO, Jannasch HW. 1981. Chemolithotrophic sulfur-oxidizing bacteria from the galapagos rift hydrothermal vents. Appl Environ Microbiol 42:317-24.
9. Gugliandolo C, Maugeria TL. 1993. Chemolithotrophic, sulfur-oxidizing bacteria from a marine, shallow hydrothermal vent of Vulcano (Italy). Geomicrobiology Journal 11:109-120.
10. Emerson D, Moyer CL. 2002. Neutrophilic Fe-oxidizing bacteria are abundant at the Loihi Seamount hydrothermal vents and play a major role in Fe oxide deposition. Appl Environ Microbiol 68:3085-93.
11. Baross JA, Hoffmann SE. 1985. Submarine hydrothermal vents and associated gradient environments as sites for the origin and evolution of life. Origins Life Evol Biosphere 15:327-345.
12. Rasmussen B. 2000. Filamentous microfossils in a 3,235-million-year-old volcanogenic massive sulphide deposit. Nature 405:676-9.
13. Stoodley P, Sauer K, Davies DG, Costerton JW. 2002. Biofilms as complex differentiated communities. Annu Rev Microbiol 56:187-209.
14. Costerton JW. 1995. Overview of microbial biofilms. J Ind Microbiol 15:137-40.
15. Yamada KJ, Kielian T. 2019. Biofilm-Leukocyte Cross-Talk: Impact on Immune Polarization and Immunometabolism. J Innate Immun 11:280-288.
16. Le KY, Park MD, Otto M. 2018. Immune Evasion Mechanisms of Staphylococcus epidermidis Biofilm Infection. Front Microbiol 9:359.

17. Gonzalez JF, Hahn MM, Gunn JS. 2018. Chronic biofilm-based infections: skewing of the immune response. Pathog Dis 76.

18. Stewart PS. 2014. Biophysics of biofilm infection. Pathog Dis 70:212-8.

19. Dragos A, Kiesewalter H, Martin M, Hsu CY, Hartmann R, Wechsler T, Eriksen C, Brix S, Drescher K, Stanley-Wall N, Kummerli R, Kovacs AT. 2018. Division of Labor during Biofilm Matrix Production. Curr Biol 28:1903-1913 e5.

20. Bisht K, Wakeman CA. 2019. Discovery and Therapeutic Targeting of Differentiated Biofilm Subpopulations. Front Microbiol 10:1908.

21. Avery SV. 2006. Microbial cell individuality and the underlying sources of heterogeneity. Nat Rev Microbiol 4:577-87.

22. Branda SS, Gonzalez-Pastor JE, Ben-Yehuda S, Losick R, Kolter R. 2001. Fruiting body formation by Bacillus subtilis. Proc Natl Acad Sci U S A 98:11621-6.

23. Kaiser D, Welch R. 2004. Dynamics of fruiting body morphogenesis. J Bacteriol 186:919-27.

24. Moormeier DE, Bayles KW. 2017. Staphylococcus aureus biofilm: a complex developmental organism. Mol Microbiol 104:365-376.

25. Moormeier DE, Bose JL, Horswill AR, Bayles KW. 2014. Temporal and stochastic control of Staphylococcus aureus biofilm development. mBio 5:e01341-14.

26. Gubner R, Beech IB. 2000. The effect of extracellular polymeric substances on the attachment of Pseudomonas NCIMB 2021 to AISI 304 and 316 stainless steel. Biofouling 15:25-36.

27. Lorite GS, Rodrigues CM, de Souza AA, Kranz C, Mizaikoff B, Cotta MA. 2011. The role of conditioning film formation and surface chemical changes on Xylella fastidiosa adhesion and biofilm evolution. J Colloid Interface Sci 359:289-95.

28. Mittelman MW. 1996. Adhesion to biomaterials. Bacterial adhesion: molecular and ecological diversity:89-127.

29. Palmer J, Flint S, Brooks J. 2007. Bacterial cell attachment, the beginning of a biofilm. J Ind Microbiol Biotechnol 34:577-88.

30. Ren Y, Wang C, Chen Z, Allan E, van der Mei HC, Busscher HJ. 2018. Emergent heterogeneous microenvironments in biofilms: substratum surface heterogeneity and bacterial adhesion force-sensing. FEMS Microbiol Rev 42:259-272.

31. Sheng X, Ting YP, Pehkonen SO. 2008. The influence of ionic strength, nutrients and pH on bacterial adhesion to metals. J Colloid Interface Sci 321:256-64.

32. Li B, Logan BE. 2004. Bacterial adhesion to glass and metal-oxide surfaces. Colloids Surf B Biointerfaces 36:81-90.

33. Hwang G, Liang J, Kang S, Tong M, Liu Y. 2013. The role of conditioning film formation in Pseudomonas aeruginosa PAO1 adhesion to inert surfaces in aquatic environments. Biochemical Engineering Journal 76:90-98.

34. Talluri SNL, Winter RM, Salem DR. 2020. Conditioning film formation and its influence on the initial adhesion and biofilm formation by a cyanobacterium on photobioreactor materials. Biofouling 36:183-199.

35. Jahnke LL, Eder W, Huber R, Hope JM, Hinrichs KU, Hayes JM, Des Marais DJ, Cady SL, Summons RE. 2001. Signature lipids and stable carbon isotope analyses of Octopus Spring hyperthermophilic communities compared with those of Aquificales representatives. Appl Environ Microbiol 67:5179-89.

36. Reysenbach AL, Banta AB, Boone DR, Cary SC, Luther GW. 2000. Microbial essentials at hydrothermal vents. Nature 404:835.

37. Hall-Stoodley L, Costerton JW, Stoodley P. 2004. Bacterial biofilms: from the natural environment to infectious diseases. Nat Rev Microbiol 2:95-108.

38. Tseng BS, Zhang W, Harrison JJ, Quach TP, Song JL, Penterman J, Singh PK, Chopp DL, Packman AI, Parsek MR. 2013. The extracellular matrix protects Pseudomonas aeruginosa biofilms by limiting the penetration of tobramycin. Environ Microbiol 15:2865-78.

39. Lewis K. 2008. Multidrug tolerance of biofilms and persister cells. Curr Top Microbiol Immunol 322:107-31.

40. Berne C, Ellison CK, Ducret A, Brun YV. 2018. Bacterial adhesion at the single-cell level. Nat Rev Microbiol 16:616-627.

41. Friedlander RS, Vlamakis H, Kim P, Khan M, Kolter R, Aizenberg J. 2013. Bacterial flagella explore microscale hummocks and hollows to increase adhesion. Proc Natl Acad Sci U S A 110:5624-9.

42. Belas R. 2014. Biofilms, flagella, and mechanosensing of surfaces by bacteria. Trends Microbiol 22:517-27.

43. Heilmann C. 2011. Adhesion mechanisms of staphylococci. Adv Exp Med Biol 715:105-23.

44. Cucarella C, Solano C, Valle J, Amorena B, Lasa I, Penades JR. 2001. Bap, a Staphylococcus aureus surface protein involved in biofilm formation. J Bacteriol 183:2888-96.

45. Abraham NM, Jefferson KK. 2012. Staphylococcus aureus clumping factor B mediates biofilm formation in the absence of calcium. Microbiology (Reading) 158:1504-1512.

46. O'Neill E, Pozzi C, Houston P, Humphreys H, Robinson DA, Loughman A, Foster TJ, O'Gara JP. 2008. A novel Staphylococcus aureus biofilm phenotype mediated by the fibronectin-binding proteins, FnBPA and FnBPB. J Bacteriol 190:3835-50.

47. Geoghegan JA, Monk IR, O'Gara JP, Foster TJ. 2013. Subdomains N2N3 of fibronectin binding protein A mediate Staphylococcus aureus biofilm formation and adherence to fibrinogen using distinct mechanisms. J Bacteriol 195:2675-83.

48. Geoghegan JA, Corrigan RM, Gruszka DT, Speziale P, O'Gara JP, Potts JR, Foster TJ. 2010. Role of surface protein SasG in biofilm formation by Staphylococcus aureus. J Bacteriol 192:5663-73.

49. Corrigan RM, Rigby D, Handley P, Foster TJ. 2007. The role of Staphylococcus aureus surface protein SasG in adherence and biofilm formation. Microbiology (Reading) 153:2435-2446.

50. Schroeder K, Jularic M, Horsburgh SM, Hirschhausen N, Neumann C, Bertling A, Schulte A, Foster S, Kehrel BE, Peters G, Heilmann C. 2009. Molecular characterization of a novel Staphylococcus aureus surface protein (SasC) involved in cell aggregation and biofilm accumulation. PLoS One 4:e7567.

51. Merino N, Toledo-Arana A, Vergara-Irigaray M, Valle J, Solano C, Calvo E, Lopez JA, Foster TJ, Penades JR, Lasa I. 2009. Protein A-mediated multicellular behavior in Staphylococcus aureus. J Bacteriol 191:832-43.

52. Feuillie C, Formosa-Dague C, Hays LM, Vervaeck O, Derclaye S, Brennan MP, Foster TJ, Geoghegan JA, Dufrene YF. 2017. Molecular interactions and inhibition of the staphylococcal biofilm-forming protein SdrC. Proc Natl Acad Sci U S A 114:3738-3743.

53. Mazmanian SK, Liu G, Ton-That H, Schneewind O. 1999. Staphylococcus aureus sortase, an enzyme that anchors surface proteins to the cell wall. Science 285:760-3.

54. Patti JM, Allen BL, McGavin MJ, Hook M. 1994. MSCRAMM-mediated adherence of microorganisms to host tissues. Annu Rev Microbiol 48:585-617.

55. Patti JM, Hook M. 1994. Microbial adhesins recognizing extracellular matrix macromolecules. Curr Opin Cell Biol 6:752-8.

56. Deivanayagam CC, Wann ER, Chen W, Carson M, Rajashankar KR, Hook M, Narayana SV. 2002. A novel variant of the immunoglobulin fold in surface adhesins of Staphylococcus aureus: crystal structure of the fibrinogen-binding MSCRAMM, clumping factor A. EMBO J 21:6660-72.

57. Foster TJ, Geoghegan JA, Ganesh VK, Hook M. 2014. Adhesion, invasion and evasion: the many functions of the surface proteins of Staphylococcus aureus. Nat Rev Microbiol 12:49-62.

58. Biswas R, Voggu L, Simon UK, Hentschel P, Thumm G, Gotz F. 2006. Activity of the major staphylococcal autolysin Atl. FEMS Microbiol Lett 259:260-8.

59. Houston P, Rowe SE, Pozzi C, Waters EM, O'Gara JP. 2011. Essential role for the major autolysin in the fibronectin-binding protein-mediated Staphylococcus aureus biofilm phenotype. Infect Immun 79:1153-65.

60. Kohler TP, Gisch N, Binsker U, Schlag M, Darm K, Volker U, Zahringer U, Hammerschmidt S. 2014. Repeating structures of the major staphylococcal autolysin are essential for the interaction with human thrombospondin 1 and vitronectin. J Biol Chem 289:4070-82.

61. Chavakis T, Wiechmann K, Preissner KT, Herrmann M. 2005. Staphylococcus aureus interactions with the endothelium: the role of bacterial "secretable expanded repertoire adhesive molecules" (SERAM) in disturbing host defense systems. Thromb Haemost 94:278-85.

62. Flemming HC, Wingender J. 2010. The biofilm matrix. Nat Rev Microbiol 8:623-33.

63. Kostakioti M, Hadjifrangiskou M, Hultgren SJ. 2013. Bacterial biofilms: development, dispersal, and therapeutic strategies in the dawn of the postantibiotic era. Cold Spring Harb Perspect Med 3:a010306.

64. Foulston L, Elsholz AK, DeFrancesco AS, Losick R. 2014. The extracellular matrix of Staphylococcus aureus biofilms comprises cytoplasmic proteins that associate with the cell surface in response to decreasing pH. mBio 5:e01667-14.

65. Graf AC, Leonard A, Schauble M, Rieckmann LM, Hoyer J, Maass S, Lalk M, Becher D, Pane-Farre J, Riedel K. 2019. Virulence Factors Produced by Staphylococcus aureus Biofilms Have a Moonlighting Function Contributing to Biofilm Integrity. Mol Cell Proteomics 18:1036-1053.

66. Stewart PS, Franklin MJ. 2008. Physiological heterogeneity in biofilms. Nat Rev Microbiol 6:199-210.

67. Cramton SE, Gerke C, Schnell NF, Nichols WW, Gotz F. 1999. The intercellular adhesion (ica) locus is present in Staphylococcus aureus and is required for biofilm formation. Infect Immun 67:5427-33.

68. Mlynek KD, Bulock LL, Stone CJ, Curran LJ, Sadykov MR, Bayles KW, Brinsmade SR. 2020. Genetic and Biochemical Analysis of CodY-Mediated Cell Aggregation in Staphylococcus aureus Reveals an Interaction between Extracellular DNA and Polysaccharide in the Extracellular Matrix. J Bacteriol 202.

69. Lei MG, Gupta RK, Lee CY. 2017. Proteomics of Staphylococcus aureus biofilm matrix in a rat model of orthopedic implant-associated infection. PLoS One 12:e0187981.

70. Shanks RM, Donegan NP, Graber ML, Buckingham SE, Zegans ME, Cheung AL, O'Toole GA. 2005. Heparin stimulates Staphylococcus aureus biofilm formation. Infect Immun 73:4596-606.

71. Ibberson CB, Parlet CP, Kwiecinski J, Crosby HA, Meyerholz DK, Horswill AR. 2016. Hyaluronan Modulation Impacts Staphylococcus aureus Biofilm Infection. Infect Immun 84:1917-1929.

72. Otto M. 2013. Staphylococcal infections: mechanisms of biofilm maturation and detachment as critical determinants of pathogenicity. Annu Rev Med 64:175-88.

73. Le KY, Dastgheyb S, Ho TV, Otto M. 2014. Molecular determinants of staphylococcal biofilm dispersal and structuring. Front Cell Infect Microbiol 4:167.

74. Moormeier DE, Endres JL, Mann EE, Sadykov MR, Horswill AR, Rice KC, Fey PD, Bayles KW. 2013. Use of microfluidic technology to analyze gene expression during Staphylococcus aureus biofilm formation reveals distinct physiological niches. Appl Environ Microbiol 79:3413-24.

75. Singh PK, Bartalomej S, Hartmann R, Jeckel H, Vidakovic L, Nadell CD, Drescher K. 2017. Vibrio cholerae Combines Individual and Collective Sensing to Trigger Biofilm Dispersal. Curr Biol 27:3359-3366 e7.

76. An S, Wu J, Zhang LH. 2010. Modulation of Pseudomonas aeruginosa biofilm dispersal by a cyclic-Di-GMP phosphodiesterase with a putative hypoxia-sensing domain. Appl Environ Microbiol 76:8160-73.

77. Li Y, Petrova OE, Su S, Lau GW, Panmanee W, Na R, Hassett DJ, Davies DG, Sauer K. 2014. BdlA, DipA and induced dispersion contribute to acute virulence and chronic persistence of Pseudomonas aeruginosa. PLoS Pathog 10:e1004168.

78. Sauer K, Cullen MC, Rickard AH, Zeef LA, Davies DG, Gilbert P. 2004. Characterization of nutrient-induced dispersion in Pseudomonas aeruginosa PAO1 biofilm. J Bacteriol 186:7312-26.

79. Gjermansen M, Ragas P, Sternberg C, Molin S, Tolker-Nielsen T. 2005. Characterization of starvation-induced dispersion in Pseudomonas putida biofilms. Environ Microbiol 7:894-906.

80. Goodwine J, Gil J, Doiron A, Valdes J, Solis M, Higa A, Davis S, Sauer K. 2019. Pyruvate-depleting conditions induce biofilm dispersion and enhance the efficacy of antibiotics in killing biofilms in vitro and in vivo. Sci Rep 9:3763.

81. Valentini M, Filloux A. 2016. Biofilms and Cyclic di-GMP (c-di-GMP) Signaling: Lessons from Pseudomonas aeruginosa and Other Bacteria. J Biol Chem 291:12547-55.

82. Hengge R. 2009. Principles of c-di-GMP signalling in bacteria. Nat Rev Microbiol 7:263-73.

83. Basu Roy A, Sauer K. 2014. Diguanylate cyclase NicD-based signalling mechanism of nutrient-induced dispersion by Pseudomonas aeruginosa. Mol Microbiol 94:771-93.

84. Sauer K, Camper AK, Ehrlich GD, Costerton JW, Davies DG. 2002. Pseudomonas aeruginosa displays multiple phenotypes during development as a biofilm. J Bacteriol 184:1140-54.

85. Rumbaugh KP, Sauer K. 2020. Biofilm dispersion. Nat Rev Microbiol 18:571-586.

86. Boles BR, Horswill AR. 2008. Agr-mediated dispersal of Staphylococcus aureus biofilms. PLoS Pathog 4:e1000052.

87. Peschel A, Otto M. 2013. Phenol-soluble modulins and staphylococcal infection. Nat Rev Microbiol 11:667-73.

88. Kiedrowski MR, Kavanaugh JS, Malone CL, Mootz JM, Voyich JM, Smeltzer MS, Bayles KW, Horswill AR. 2011. Nuclease modulates biofilm formation in community-associated methicillin-resistant Staphylococcus aureus. PLoS One 6:e26714.

89. Dubnau D, Losick R. 2006. Bistability in bacteria. Mol Microbiol 61:564-72.

90. Russell JR, Cabeen MT, Wiggins PA, Paulsson J, Losick R. 2017. Noise in a phosphorelay drives stochastic entry into sporulation in Bacillus subtilis. EMBO J 36:2856-2869.

91. van Sinderen D, Luttinger A, Kong L, Dubnau D, Venema G, Hamoen L. 1995. comK encodes the competence transcription factor, the key regulatory protein for competence development in Bacillus subtilis. Mol Microbiol 15:455-62.

92. Smits WK, Eschevins CC, Susanna KA, Bron S, Kuipers OP, Hamoen LW. 2005. Stripping Bacillus: ComK auto-stimulation is responsible for the bistable response in competence development. Mol Microbiol 56:604-14.

93. Maamar H, Dubnau D. 2005. Bistability in the Bacillus subtilis K-state (competence) system requires a positive feedback loop. Mol Microbiol 56:615-24.

94. Leisner M, Stingl K, Radler JO, Maier B. 2007. Basal expression rate of comK sets a 'switching-window' into the K-state of Bacillus subtilis. Mol Microbiol 63:1806-16.

95. Hoa TT, Tortosa P, Albano M, Dubnau D. 2002. Rok (YkuW) regulates genetic competence in Bacillus subtilis by directly repressing comK. Mol Microbiol 43:15-26.

96. Hamoen LW, Venema G, Kuipers OP. 2003. Controlling competence in Bacillus subtilis: shared use of regulators. Microbiology (Reading) 149:9-17.

97. Hamoen LW, Van Werkhoven AF, Venema G, Dubnau D. 2000. The pleiotropic response regulator DegU functions as a priming protein in competence development in Bacillus subtilis. Proc Natl Acad Sci U S A 97:9246-51.

98. Serror P, Sonenshein AL. 1996. CodY is required for nutritional repression of Bacillus subtilis genetic competence. J Bacteriol 178:5910-5.

99. Mirouze N, Desai Y, Raj A, Dubnau D. 2012. Spo0A~P imposes a temporal gate for the bimodal expression of competence in Bacillus subtilis. PLoS Genet 8:e1002586.

100. Smits WK, Bongiorni C, Veening JW, Hamoen LW, Kuipers OP, Perego M. 2007. Temporal separation of distinct differentiation pathways by a dual specificity Rap-Phr system in Bacillus subtilis. Mol Microbiol 65:103-20.

101. Ogura M, Tanaka T. 1996. Bacillus subtilis DegU acts as a positive regulator for comK expression. FEBS Lett 397:173-6.

102. Turgay K, Hahn J, Burghoorn J, Dubnau D. 1998. Competence in Bacillus subtilis is controlled by regulated proteolysis of a transcription factor. EMBO J 17:6730-8.

103. Turgay K, Hamoen LW, Venema G, Dubnau D. 1997. Biochemical characterization of a molecular switch involving the heat shock protein ClpC, which controls the activity of ComK, the competence transcription factor of Bacillus subtilis. Genes Dev 11:119-28.

104. D'Souza C, Nakano MM, Zuber P. 1994. Identification of comS, a gene of the srfA operon that regulates the establishment of genetic competence in Bacillus subtilis. Proc Natl Acad Sci U S A 91:9397-401.

105. Gamba P, Jonker MJ, Hamoen LW. 2015. A Novel Feedback Loop That Controls Bimodal Expression of Genetic Competence. PLoS Genet 11:e1005047.

106. Haijema BJ, Hahn J, Haynes J, Dubnau D. 2001. A ComGA-dependent checkpoint limits growth during the escape from competence. Mol Microbiol 40:52-64.

107. Briley K, Jr., Dorsey-Oresto A, Prepiak P, Dias MJ, Mann JM, Dubnau D. 2011. The secretion ATPase ComGA is required for the binding and transport of transforming DNA. Mol Microbiol 81:818-30.

108. Kussell E, Leibler S. 2005. Phenotypic diversity, population growth, and information in fluctuating environments. Science 309:2075-8.

109. DelMain EA, Moormeier DE, Endres JL, Hodges RE, Sadykov MR, Horswill AR, Bayles KW. 2020. Stochastic Expression of Sae-Dependent Virulence Genes during Staphylococcus aureus Biofilm Development Is Dependent on SaeS. mBio 11.

110. Simm R, Morr M, Kader A, Nimtz M, Romling U. 2004. GGDEF and EAL domains inversely regulate cyclic di-GMP levels and transition from sessility to motility. Mol Microbiol 53:1123-34.

111. Romling U, Galperin MY, Gomelsky M. 2013. Cyclic di-GMP: the first 25 years of a universal bacterial second messenger. Microbiol Mol Biol Rev 77:1-52.

112. Armbruster CR, Lee CK, Parker-Gilham J, de Anda J, Xia A, Zhao K, Murakami K, Tseng BS, Hoffman LR, Jin F, Harwood CS, Wong GC, Parsek MR. 2019. Heterogeneity in surface sensing suggests a division of labor in Pseudomonas aeruginosa populations. Elife 8.

113. Serra DO, Hengge R. 2019. A c-di-GMP-Based Switch Controls Local Heterogeneity of Extracellular Matrix Synthesis which Is Crucial for Integrity and Morphogenesis of Escherichia coli Macrocolony Biofilms. J Mol Biol 431:4775-4793.

114. Weber H, Pesavento C, Possling A, Tischendorf G, Hengge R. 2006. Cyclic-di-GMP-mediated signalling within the sigma network of Escherichia coli. Mol Microbiol 62:1014-34.

115. Pesavento C, Becker G, Sommerfeldt N, Possling A, Tschowri N, Mehlis A, Hengge R. 2008. Inverse regulatory coordination of motility and curli-mediated adhesion in Escherichia coli. Genes Dev 22:2434-46.

116. Lindenberg S, Klauck G, Pesavento C, Klauck E, Hengge R. 2013. The EAL domain protein YciR acts as a trigger enzyme in a c-di-GMP signalling cascade in E. coli biofilm control. EMBO J 32:2001-14.

117. Serra DO, Hengge R. 2014. Stress responses go three dimensional - the spatial order of physiological differentiation in bacterial macrocolony biofilms. Environ Microbiol 16:1455-71.

118. Klauck G, Serra DO, Possling A, Hengge R. 2018. Spatial organization of different sigma factor activities and c-di-GMP signalling within the three-dimensional landscape of a bacterial biofilm. Open Biol 8.

119. Hengge R. 2016. Trigger phosphodiesterases as a novel class of c-di-GMP effector proteins. Philos Trans R Soc Lond B Biol Sci 371.

120. Fitzgerald DM, Bonocora RP, Wade JT. 2014. Comprehensive mapping of the Escherichia coli flagellar regulatory network. PLoS Genet 10:e1004649.

121. Serra DO, Richter AM, Hengge R. 2013. Cellulose as an architectural element in spatially structured Escherichia coli biofilms. J Bacteriol 195:5540-54.

122. Serra DO, Richter AM, Klauck G, Mika F, Hengge R. 2013. Microanatomy at cellular resolution and spatial order of physiological differentiation in a bacterial biofilm. mBio 4:e00103-13.

123. Stover AG, Driks A. 1999. Regulation of synthesis of the Bacillus subtilis transition-phase, spore-associated antibacterial protein TasA. J Bacteriol 181:5476-81.

124. Irie Y, Borlee BR, O'Connor JR, Hill PJ, Harwood CS, Wozniak DJ, Parsek MR. 2012. Self-produced exopolysaccharide is a signal that stimulates biofilm formation in Pseudomonas aeruginosa. Proc Natl Acad Sci U S A 109:20632-6.

125. Elsholz AK, Wacker SA, Losick R. 2014. Self-regulation of exopolysaccharide production in Bacillus subtilis by a tyrosine kinase. Genes Dev 28:1710-20.

126. Kavanaugh JS, Flack CE, Lister J, Ricker EB, Ibberson CB, Jenul C, Moormeier DE, Delmain EA, Bayles KW, Horswill AR. 2019. Identification of Extracellular DNA-Binding Proteins in the Biofilm Matrix. mBio 10.

127. Kim D, Koo H. 2020. Spatial Design of Polymicrobial Oral Biofilm in Its Native Disease State. J Dent Res 99:597-603.

128. Lawrence JR, Swerhone GD, Kuhlicke U, Neu TR. 2016. In situ evidence for metabolic and chemical microdomains in the structured polymer matrix of bacterial microcolonies. FEMS Microbiol Ecol 92.

129. Williamson KS, Richards LA, Perez-Osorio AC, Pitts B, McInnerney K, Stewart PS, Franklin MJ. 2012. Heterogeneity in Pseudomonas aeruginosa biofilms includes expression of ribosome hibernation factors in the antibiotic-tolerant subpopulation and hypoxia-induced stress response in the metabolically active population. J Bacteriol 194:2062-73.

130. Oshima T, Aiba H, Masuda Y, Kanaya S, Sugiura M, Wanner BL, Mori H, Mizuno T. 2002. Transcriptome analysis of all two-component regulatory system mutants of Escherichia coli K-12. Mol Microbiol 46:281-91.

131. Walters MC, 3rd, Roe F, Bugnicourt A, Franklin MJ, Stewart PS. 2003. Contributions of antibiotic penetration, oxygen limitation, and low metabolic activity to tolerance of Pseudomonas aeruginosa biofilms to ciprofloxacin and tobramycin. Antimicrob Agents Chemother 47:317-23.

132. Beebout CJ, Eberly AR, Werby SH, Reasoner SA, Brannon JR, De S, Fitzgerald MJ, Huggins MM, Clayton DB, Cegelski L, Hadjifrangiskou M. 2019. Respiratory Heterogeneity Shapes Biofilm Formation and Host Colonization in Uropathogenic Escherichia coli. mBio 10.

133. Yung YP, McGill SL, Chen H, Park H, Carlson RP, Hanley L. 2019. Reverse diauxie phenotype in Pseudomonas aeruginosa biofilm revealed by exometabolomics and label-free proteomics. NPJ Biofilms Microbiomes 5:31.

134. Borriello G, Werner E, Roe F, Kim AM, Ehrlich GD, Stewart PS. 2004. Oxygen limitation contributes to antibiotic tolerance of Pseudomonas aeruginosa in biofilms. Antimicrob Agents Chemother 48:2659-64.

135. Wessel AK, Arshad TA, Fitzpatrick M, Connell JL, Bonnecaze RT, Shear JB, Whiteley M. 2014. Oxygen limitation within a bacterial aggregate. mBio 5:e00992.

136. Yang SJ, Rice KC, Brown RJ, Patton TG, Liou LE, Park YH, Bayles KW. 2005. A LysR-type regulator, CidR, is required for induction of the Staphylococcus aureus cidABC operon. J Bacteriol 187:5893-900.

137. Sharma-Kuinkel BK, Mann EE, Ahn JS, Kuechenmeister LJ, Dunman PM, Bayles KW. 2009. The Staphylococcus aureus LytSR two-component regulatory system affects biofilm formation. J Bacteriol 191:4767-75.

138. Yang SJ, Dunman PM, Projan SJ, Bayles KW. 2006. Characterization of the Staphylococcus aureus CidR regulon: elucidation of a novel role for acetoin metabolism in cell death and lysis. Mol Microbiol 60:458-68.

139. Lehman MK, Bose JL, Sharma-Kuinkel BK, Moormeier DE, Endres JL, Sadykov MR, Biswas I, Bayles KW. 2015. Identification of the amino acids essential for LytSR-mediated signal transduction in Staphylococcus aureus and their roles in biofilm-specific gene expression. Mol Microbiol 95:723-37.

140. Brauner A, Fridman O, Gefen O, Balaban NQ. 2016. Distinguishing between resistance, tolerance and persistence to antibiotic treatment. Nat Rev Microbiol 14:320-30.

141. Hobby GL. 1944. The Antibacterial Action of Penicillin against Gram Negative Organisms. Science 100:500-1.

142. Bigger JW. 1944. Treatment of Staphylococcal Infections with Penicillin. The Lancet 244:497-500.

143. Fisher RA, Gollan B, Helaine S. 2017. Persistent bacterial infections and persister cells. Nat Rev Microbiol 15:453-464.

144. Reygaert WC. 2018. An overview of the antimicrobial resistance mechanisms of bacteria. AIMS Microbiol 4:482-501.

145. Levin BR. 2004. Microbiology. Noninherited resistance to antibiotics. Science 305:1578-9.

146. Lewis K. 2007. Persister cells, dormancy and infectious disease. Nat Rev Microbiol 5:48-56.

147. Dawson CC, Intapa C, Jabra-Rizk MA. 2011. "Persisters": survival at the cellular level. PLoS Pathog 7:e1002121.

148. Kussell E, Kishony R, Balaban NQ, Leibler S. 2005. Bacterial persistence: a model of survival in changing environments. Genetics 169:1807-14.

149. Beaumont HJ, Gallie J, Kost C, Ferguson GC, Rainey PB. 2009. Experimental evolution of bet hedging. Nature 462:90-3.

150. Spoering AL, Lewis K. 2001. Biofilms and planktonic cells of Pseudomonas aeruginosa have similar resistance to killing by antimicrobials. J Bacteriol 183:6746-51.

151. Shah D, Zhang Z, Khodursky A, Kaldalu N, Kurg K, Lewis K. 2006. Persisters: a distinct physiological state of E. coli. BMC Microbiol 6:53.

152. Kwan BW, Valenta JA, Benedik MJ, Wood TK. 2013. Arrested protein synthesis increases persister-like cell formation. Antimicrob Agents Chemother 57:1468-73.

153. Jayaraman R. 2008. Bacterial persistence: some new insights into an old phenomenon. J Biosci 33:795-805.

154. Ronneau S, Helaine S. 2019. Clarifying the Link between Toxin-Antitoxin Modules and Bacterial Persistence. J Mol Biol 431:3462-3471.

155. Schuster CF, Bertram R. 2013. Toxin-antitoxin systems are ubiquitous and versatile modulators of prokaryotic cell fate. FEMS Microbiol Lett 340:73-85.

156. Van Melderen L, Saavedra De Bast M. 2009. Bacterial toxin-antitoxin systems: more than selfish entities? PLoS Genet 5:e1000437.

157. Moyed HS, Bertrand KP. 1983. hipA, a newly recognized gene of Escherichia coli K-12 that affects frequency of persistence after inhibition of murein synthesis. J Bacteriol 155:768-75.

158. Black DS, Irwin B, Moyed HS. 1994. Autoregulation of hip, an operon that affects lethality due to inhibition of peptidoglycan or DNA synthesis. J Bacteriol 176:4081-91.

159. Evdokimov A, Voznesensky I, Fennell K, Anderson M, Smith JF, Fisher DA. 2009. New kinase regulation mechanism found in HipBA: a bacterial persistence switch. Acta Crystallogr D Biol Crystallogr 65:875-9.

160. Germain E, Castro-Roa D, Zenkin N, Gerdes K. 2013. Molecular mechanism of bacterial persistence by HipA. Mol Cell 52:248-54.

161. Germain E, Roghanian M, Gerdes K, Maisonneuve E. 2015. Stochastic induction of persister cells by HipA through (p)ppGpp-mediated activation of mRNA endonucleases. Proc Natl Acad Sci U S A 112:5171-6.

162. Kaspy I, Rotem E, Weiss N, Ronin I, Balaban NQ, Glaser G. 2013. HipA-mediated antibiotic persistence via phosphorylation of the glutamyl-tRNA-synthetase. Nat Commun 4:3001.

163. Black DS, Kelly AJ, Mardis MJ, Moyed HS. 1991. Structure and organization of hip, an operon that affects lethality due to inhibition of peptidoglycan or DNA synthesis. J Bacteriol 173:5732-9.

164. Schumacher MA, Piro KM, Xu W, Hansen S, Lewis K, Brennan RG. 2009. Molecular mechanisms of HipA-mediated multidrug tolerance and its neutralization by HipB. Science 323:396-401.

165. Schumacher MA, Balani P, Min J, Chinnam NB, Hansen S, Vulic M, Lewis K, Brennan RG. 2015. HipBA-promoter structures reveal the basis of heritable multidrug tolerance. Nature 524:59-64.

166. Hansen S, Vulic M, Min J, Yen TJ, Schumacher MA, Brennan RG, Lewis K. 2012. Regulation of the Escherichia coli HipBA toxin-antitoxin system by proteolysis. PLoS One 7:e39185.

167. Lou C, Li Z, Ouyang Q. 2008. A molecular model for persister in E. coli. J Theor Biol 255:205-9.

168. Fasani RA, Savageau MA. 2013. Molecular mechanisms of multiple toxin-antitoxin systems are coordinated to govern the persister phenotype. Proc Natl Acad Sci U S A 110:E2528-37.

169. Feng J, Kessler DA, Ben-Jacob E, Levine H. 2014. Growth feedback as a basis for persister bistability. Proc Natl Acad Sci U S A 111:544-9.

170. Gelens L, Hill L, Vandervelde A, Danckaert J, Loris R. 2013. A general model for toxin-antitoxin module dynamics can explain persister cell formation in E. coli. PLoS Comput Biol 9:e1003190.

171. Van den Bergh B, Fauvart M, Michiels J. 2017. Formation, physiology, ecology, evolution and clinical importance of bacterial persisters. FEMS Microbiol Rev 41:219-251.

172. Wood TK, Knabel SJ, Kwan BW. 2013. Bacterial persister cell formation and dormancy. Appl Environ Microbiol 79:7116-21.

173. Potrykus K, Cashel M. 2008. (p)ppGpp: still magical? Annu Rev Microbiol 62:35-51.

174. Srivatsan A, Wang JD. 2008. Control of bacterial transcription, translation and replication by (p)ppGpp. Curr Opin Microbiol 11:100-5.

175. Balaban NQ, Merrin J, Chait R, Kowalik L, Leibler S. 2004. Bacterial persistence as a phenotypic switch. Science 305:1622-5.

176. Rotem E, Loinger A, Ronin I, Levin-Reisman I, Gabay C, Shoresh N, Biham O, Balaban NQ. 2010. Regulation of phenotypic variability by a threshold-based mechanism underlies bacterial persistence. Proc Natl Acad Sci U S A 107:12541-6.

177. Pu Y, Zhao Z, Li Y, Zou J, Ma Q, Zhao Y, Ke Y, Zhu Y, Chen H, Baker MAB, Ge H, Sun Y, Xie XS, Bai F. 2016. Enhanced Efflux Activity Facilitates Drug Tolerance in Dormant Bacterial Cells. Mol Cell 62:284-294.

178. Sanchez-Romero MA, Casadesus J. 2014. Contribution of phenotypic heterogeneity to adaptive antibiotic resistance. Proc Natl Acad Sci U S A 111:355-60.

179. Aldridge BB, Fernandez-Suarez M, Heller D, Ambravaneswaran V, Irimia D, Toner M, Fortune SM. 2012. Asymmetry and aging of mycobacterial cells lead to variable growth and antibiotic susceptibility. Science 335:100-4.

180. Salgado-Pabon W, Schlievert PM. 2014. Models matter: the search for an effective Staphylococcus aureus vaccine. Nat Rev Microbiol 12:585-91.

181. Somerville GA, Proctor RA. 2009. At the crossroads of bacterial metabolism and virulence factor synthesis in Staphylococci. Microbiol Mol Biol Rev 73:233-48.

182. Mazharul Islam M, Thomas VC, Van Beek M, Ahn JS, Alqarzaee AA, Zhou C, Fey PD, Bayles KW, Saha R. 2020. An integrated computational and experimental study to investigate Staphylococcus aureus metabolism. NPJ Syst Biol Appl 6:3.

183. Waters NR, Samuels DJ, Behera RK, Livny J, Rhee KY, Sadykov MR, Brinsmade SR. 2016. A spectrum of CodY activities drives metabolic reorganization and virulence gene expression in Staphylococcus aureus. Mol Microbiol 101:495-514.

184. Kaiser JC, King AN, Grigg JC, Sheldon JR, Edgell DR, Murphy MEP, Brinsmade SR, Heinrichs DE. 2018. Repression of branched-chain amino acid synthesis in Staphylococcus aureus is mediated by isoleucine via CodY, and by a leucine-rich attenuator peptide. PLoS Genet 14:e1007159.

185. Majerczyk CD, Dunman PM, Luong TT, Lee CY, Sadykov MR, Somerville GA, Bodi K, Sonenshein AL. 2010. Direct targets of CodY in Staphylococcus aureus. J Bacteriol 192:2861-77.

186. Brinsmade SR. 2017. CodY, a master integrator of metabolism and virulence in Gram-positive bacteria. Curr Genet 63:417-425.

187. Majerczyk CD, Sadykov MR, Luong TT, Lee C, Somerville GA, Sonenshein AL. 2008. Staphylococcus aureus CodY negatively regulates virulence gene expression. J Bacteriol 190:2257-65.

188. Tu Quoc PH, Genevaux P, Pajunen M, Savilahti H, Georgopoulos C, Schrenzel J, Kelley WL. 2007. Isolation and characterization of biofilm formation-defective mutants of Staphylococcus aureus. Infect Immun 75:1079-88.

189. Atwood DN, Loughran AJ, Courtney AP, Anthony AC, Meeker DG, Spencer HJ, Gupta RK, Lee CY, Beenken KE, Smeltzer MS. 2015. Comparative impact of diverse regulatory loci on Staphylococcus aureus biofilm formation. Microbiologyopen 4:436-51.

190. Lorca GL, Chung YJ, Barabote RD, Weyler W, Schilling CH, Saier MH, Jr. 2005. Catabolite repression and activation in Bacillus subtilis: dependency on CcpA, HPr, and HprK. J Bacteriol 187:7826-39.

191. Gorke B, Stulke J. 2008. Carbon catabolite repression in bacteria: many ways to make the most out of nutrients. Nat Rev Microbiol 6:613-24.

192. Poudel S, Tsunemoto H, Seif Y, Sastry AV, Szubin R, Xu S, Machado H, Olson CA, Anand A, Pogliano J, Nizet V, Palsson BO. 2020. Revealing 29 sets of independently modulated genes in Staphylococcus aureus, their regulators, and role in key physiological response. Proc Natl Acad Sci U S A 117:17228-17239.

193. Wunsche A, Hammer E, Bartholomae M, Volker U, Burkovski A, Seidel G, Hillen W. 2012. CcpA forms complexes with CodY and RpoA in Bacillus subtilis. FEBS J 279:2201-14.

194. Presecan-Siedel E, Galinier A, Longin R, Deutscher J, Danchin A, Glaser P, Martin-Verstraete I. 1999. Catabolite regulation of the pta gene as part of carbon flow pathways in Bacillus subtilis. J Bacteriol 181:6889-97.

195. Seidl K, Muller S, Francois P, Kriebitzsch C, Schrenzel J, Engelmann S, Bischoff M, Berger-Bachi B. 2009. Effect of a glucose impulse on the CcpA regulon in Staphylococcus aureus. BMC Microbiol 9:95.

196. Seidl K, Goerke C, Wolz C, Mack D, Berger-Bachi B, Bischoff M. 2008. Staphylococcus aureus CcpA affects biofilm formation. Infect Immun 76:2044-50.

197. Sadykov MR, Hartmann T, Mattes TA, Hiatt M, Jann NJ, Zhu Y, Ledala N, Landmann R, Herrmann M, Rohde H, Bischoff M, Somerville GA. 2011. CcpA coordinates central metabolism and biofilm formation in Staphylococcus epidermidis. Microbiology (Reading) 157:3458-3468.

198. Shivers RP, Dineen SS, Sonenshein AL. 2006. Positive regulation of Bacillus subtilis ackA by CodY and CcpA: establishing a potential hierarchy in carbon flow. Mol Microbiol 62:811-22.

199. Seidl K, Stucki M, Ruegg M, Goerke C, Wolz C, Harris L, Berger-Bachi B, Bischoff M. 2006. Staphylococcus aureus CcpA affects virulence determinant production and antibiotic resistance. Antimicrob Agents Chemother 50:1183-94.

200. Hanahan D. 1983. Studies on transformation of Escherichia coli with plasmids. J Mol Biol 166:557-80.

201. Kreiswirth BN, Lofdahl S, Betley MJ, O'Reilly M, Schlievert PM, Bergdoll MS, Novick RP. 1983. The toxic shock syndrome exotoxin structural gene is not detectably transmitted by a prophage. Nature 305:709-12.

202. Gillaspy AF, Hickmon SG, Skinner RA, Thomas JR, Nelson CL, Smeltzer MS. 1995. Role of the accessory gene regulator (agr) in pathogenesis of staphylococcal osteomyelitis. Infect Immun 63:3373-80.

203. Sadykov MR, Windham IH, Widhelm TJ, Yajjala VK, Watson SM, Endres JL, Bavari AI, Thomas VC, Bose JL, Bayles KW. 2019. CidR and CcpA Synergistically Regulate Staphylococcus aureus cidABC Expression. J Bacteriol 201.

204. Novick RP. 1991. Genetic systems in staphylococci. Methods Enzymol 204:587-636.

205. Halsey CR, Lei S, Wax JK, Lehman MK, Nuxoll AS, Steinke L, Sadykov M, Powers R, Fey PD. 2017. Amino Acid Catabolism in Staphylococcus aureus and the Function of Carbon Catabolite Repression. mBio 8.

206. Sadykov MR, Thomas VC, Marshall DD, Wenstrom CJ, Moormeier DE, Widhelm TJ, Nuxoll AS, Powers R, Bayles KW. 2013. Inactivation of the Pta-AckA pathway causes cell death in Staphylococcus aureus. J Bacteriol 195:3035-44.

207. Nicholson WL. 2008. The Bacillus subtilis ydjL (bdhA) gene encodes acetoin reductase/2,3-butanediol dehydrogenase. Appl Environ Microbiol 74:6832-8.

208. Zeppa G, Conterno L, Gerbi V. 2001. Determination of organic acids, sugars, diacetyl, and acetoin in cheese by high-performance liquid chromatography. J Agric Food Chem 49:2722-6.

209. Liebeke M, Dorries K, Meyer H, Lalk M. 2012. Metabolome analysis of gram-positive bacteria such as Staphylococcus aureus by GC-MS and LC-MS. Methods Mol Biol 815:377-98.

210. Sadykov MR, Olson ME, Halouska S, Zhu Y, Fey PD, Powers R, Somerville GA. 2008. Tricarboxylic acid cycle-dependent regulation of Staphylococcus epidermidis polysaccharide intercellular adhesin synthesis. J Bacteriol 190:7621-32.

211. Schmittgen TD, Livak KJ. 2008. Analyzing real-time PCR data by the comparative C(T) method. Nat Protoc 3:1101-8.

212. Xu KD, Stewart PS, Xia F, Huang CT, McFeters GA. 1998. Spatial physiological heterogeneity in Pseudomonas aeruginosa biofilm is determined by oxygen availability. Appl Environ Microbiol 64:4035-9.

213. Gray CT, Wimpenny JW, Mossman MR. 1966. Regulation of metabolism in facultative bacteria. II. Effects of aerobiosis, anaerobiosis and nutrition on the formation of Krebs cycle enzymes in Escherichia coli. Biochim Biophys Acta 117:33-41.

214. Amarasingham CR, Davis BD. 1965. Regulation of alpha-ketoglutarate dehydrogenase formation in Escherichia coli. J Biol Chem 240:3664-8.

215. Fuchs S, Pane-Farre J, Kohler C, Hecker M, Engelmann S. 2007. Anaerobic gene expression in Staphylococcus aureus. J Bacteriol 189:4275-89.

216. Kim HJ, Roux A, Sonenshein AL. 2002. Direct and indirect roles of CcpA in regulation of Bacillus subtilis Krebs cycle genes. Mol Microbiol 45:179-90.

217. Blencke HM, Homuth G, Ludwig H, Mader U, Hecker M, Stulke J. 2003. Transcriptional profiling of gene expression in response to glucose in Bacillus subtilis: regulation of the central metabolic pathways. Metab Eng 5:133-49.

218. Tobisch S, Zuhlke D, Bernhardt J, Stulke J, Hecker M. 1999. Role of CcpA in regulation of the central pathways of carbon catabolism in Bacillus subtilis. J Bacteriol 181:6996-7004.

219. Somerville GA, Chaussee MS, Morgan CI, Fitzgerald JR, Dorward DW, Reitzer LJ, Musser JM. 2002. Staphylococcus aureus aconitase inactivation unexpectedly inhibits post-exponential-phase growth and enhances stationary-phase survival. Infect Immun 70:6373-82.

220. Becker P, Hufnagle W, Peters G, Herrmann M. 2001. Detection of differential gene expression in biofilm-forming versus planktonic populations of Staphylococcus aureus using micro-representational-difference analysis. Appl Environ Microbiol 67:2958-65.

221. Dumitrache A, Klingeman DM, Natzke J, Rodriguez M, Jr., Giannone RJ, Hettich RL, Davison BH, Brown SD. 2017. Specialized activities and expression differences for Clostridium thermocellum biofilm and planktonic cells. Sci Rep 7:43583.

222. Bernbom N, Vogel BF, Gram L. 2011. Listeria monocytogenes survival of UV-C radiation is enhanced by presence of sodium chloride, organic food material and by bacterial biofilm formation. Int J Food Microbiol 147:69-73.

223. Gagliano MC, Ismail SB, Stams AJM, Plugge CM, Temmink H, Van Lier JB. 2017. Biofilm formation and granule properties in anaerobic digestion at high salinity. Water Res 121:61-71.

224. Fong JC, Yildiz FH. 2008. Interplay between cyclic AMP-cyclic AMP receptor protein and cyclic di-GMP signaling in Vibrio cholerae biofilm formation. J Bacteriol 190:6646-59.

225. Smith DR, Maestre-Reyna M, Lee G, Gerard H, Wang AH, Watnick PI. 2015. In situ proteolysis of the Vibrio cholerae matrix protein RbmA promotes biofilm recruitment. Proc Natl Acad Sci U S A 112:10491-6.

226. Yin W, Wang Y, Liu L, He J. 2019. Biofilms: The Microbial "Protective Clothing" in Extreme Environments. Int J Mol Sci 20.

227. Stewart PS. 2015. Antimicrobial Tolerance in Biofilms. Microbiol Spectr 3.

228. Boles BR, Thoendel M, Singh PK. 2005. Genetic variation in biofilms and the insurance effects of diversity. Microbiology (Reading) 151:2816-2818.

229. Tong SY, Davis JS, Eichenberger E, Holland TL, Fowler VG, Jr. 2015. Staphylococcus aureus infections: epidemiology, pathophysiology, clinical manifestations, and management. Clin Microbiol Rev 28:603-61.

230. Tacconelli E, Carrara E, Savoldi A, Harbarth S, Mendelson M, Monnet DL, Pulcini C, Kahlmeter G, Kluytmans J, Carmeli Y, Ouellette M, Outterson K, Patel J, Cavaleri M, Cox EM, Houchens CR, Grayson ML, Hansen P, Singh N, Theuretzbacher U, Magrini N, Group WHOPPLW. 2018. Discovery, research, and development of new antibiotics: the WHO priority list of antibiotic-resistant bacteria and tuberculosis. Lancet Infect Dis 18:318-327.

231. Levdikov VM, Blagova E, Young VL, Belitsky BR, Lebedev A, Sonenshein AL, Wilkinson AJ. 2017. Structure of the Branched-chain Amino Acid and GTP-sensing Global Regulator, CodY, from Bacillus subtilis. J Biol Chem 292:2714-2728.

232. Domingue G, Costerton JW, Brown MR. 1996. Bacterial doubling time modulates the effects of opsonisation and available iron upon interactions between Staphylococcus aureus and human neutrophils. FEMS Immunol Med Microbiol 16:223-8.

233. Lindgren JK, Thomas VC, Olson ME, Chaudhari SS, Nuxoll AS, Schaeffer CR, Lindgren KE, Jones J, Zimmerman MC, Dunman PM, Bayles KW, Fey PD. 2014. Arginine deiminase in Staphylococcus epidermidis functions to augment biofilm maturation through pH homeostasis. J Bacteriol 196:2277-89.

234. Turinsky AJ, Moir-Blais TR, Grundy FJ, Henkin TM. 2000. Bacillus subtilis ccpA gene mutants specifically defective in activation of acetoin biosynthesis. J Bacteriol 182:5611-4.

235. Endo T, Uratani B, Freese E. 1983. Purine salvage pathways of Bacillus subtilis and effect of guanine on growth of GMP reductase mutants. J Bacteriol 155:169-79.

236. Stincone A, Prigione A, Cramer T, Wamelink MM, Campbell K, Cheung E, Olin-Sandoval V, Gruning NM, Kruger A, Tauqeer Alam M, Keller MA, Breitenbach M, Brindle KM, Rabinowitz JD, Ralser M. 2015. The return of metabolism: biochemistry and physiology of the pentose phosphate pathway. Biol Rev Camb Philos Soc 90:927-63.

237. (ed). 2014. Microbial Biochemistry. Springer Netherlands : Imprint: Springer,, Dordrecht. Accessed

238. Novick RP. 2003. Autoinduction and signal transduction in the regulation of staphylococcal virulence. Mol Microbiol 48:1429-49.

239. Roux A, Todd DA, Velazquez JV, Cech NB, Sonenshein AL. 2014. CodY-mediated regulation of the Staphylococcus aureus Agr system integrates nutritional and population density signals. J Bacteriol 196:1184-96.

240. Smith JL, Zaluzec EJ, Wery JP, Niu L, Switzer RL, Zalkin H, Satow Y. 1994. Structure of the allosteric regulatory enzyme of purine biosynthesis. Science 264:1427-33.

241. Iyer R, Baliga NS, Camilli A. 2005. Catabolite control protein A (CcpA) contributes to virulence and regulation of sugar metabolism in Streptococcus pneumoniae. J Bacteriol 187:8340-9.

242. Okshevsky M, Meyer RL. 2014. Evaluation of fluorescent stains for visualizing extracellular DNA in biofilms. J Microbiol Methods 105:102-4.

243. Warner JB, Lolkema JS. 2003. CcpA-dependent carbon catabolite repression in bacteria. Microbiol Mol Biol Rev 67:475-90.

244. Haas SE, Hooten MB, Rizzo DM, Meentemeyer RK. 2011. Forest species diversity reduces disease risk in a generalist plant pathogen invasion. Ecol Lett 14:1108-16.